

# Math-Net.Ru

Общероссийский математический портал

G. Yu. Panina, I. Streinu, Virtual polytopes, *Russian Mathematical Surveys*, 2015, Volume 70, Issue 6, 1105–1165

DOI: 10.1070/RM2015v070n06ABEH004975

Использование Общероссийского математического портала Math-Net.Ru подразумевает, что вы прочитали и согласны с пользовательским соглашением <http://www.mathnet.ru/rus/agreement>

Параметры загрузки:

IP: 18.191.205.149

10 января 2025 г., 07:06:03



# Virtual polytopes

G. Yu. Panina and I. Streinu

**Abstract.** Originating in diverse branches of mathematics, from polytope algebra and toric varieties to the theory of stressed graphs, virtual polytopes represent a natural algebraic generalization of convex polytopes. Introduced as elements of the Grothendieck group associated to the semigroup of convex polytopes, they admit a variety of geometrizations. The present survey connects the theory of virtual polytopes with other geometrical subjects, describes a series of geometrizations together with relations between them, and gives a selection of applications.

Bibliography: 50 titles.

**Keywords:** Minkowski difference, coloured polygon, polytopal function, support functions, stressed graph, McMullen’s polytope algebra, Maxwell polytope.

## Contents

1. Introduction	1106
2. Main definition	1108
2.1. Convex polytopes and Minkowski addition	1108
2.2. Virtual polytopes as the Grothendieck group	1110
2.3. Facial structure of virtual polytopes	1111
3. Virtual polytopes in dimension two	1113
3.1. The group of virtual polygons: geometric representations	1114
3.2. Examples of virtual polygons	1116
3.3. Uncoloured virtual polygons	1117
4. Virtual polytopes in arbitrary dimension	1119
4.1. The algebra of polytopal functions	1119
4.2. McMullen’s polytope algebra	1122
4.3. Support functions	1126
4.4. The combinatorial Picard group: systems of translated cones	1131

---

This work received support from Mathematisches Forschungsinstitut Oberwolfach, programmes Research-in-Pairs (2009, 2014), the National Science Foundation, Smith College, and the Euler International Mathematical Institute (St. Petersburg).

AMS 2010 *Mathematics Subject Classification.* Primary 52B11, 52B70, 14M25.

5. Virtual polytopes in dimension three	1135
5.1. Virtual polytopes as spherical stressed graphs	1135
5.2. Virtual polytopes represented by Maxwell polytopes	1138
5.3. Detecting virtual polytopes	1143
5.4. Examples of virtual polytopes in dimension three	1144
5.5. Support functions and liftings of stressed graphs	1145
6. Applications	1149
6.1. A. D. Alexandrov's problem and hyperbolic virtual polytopes	1149
6.2. Valuations of virtual polytopes. Volume and count of integer points	1153
6.3. Mixed volumes of virtual polytopes	1156
6.4. Minkowski decomposition of polytopes	1157
6.5. Projective toric varieties, Picard group, and Riemann–Roch Theorem	1159
7. Concluding remarks	1161
Bibliography	1162

## 1. Introduction

Convex polytopes in a Euclidean space form a semigroup with respect to Minkowski addition. This semigroup is not a group, since in most cases the Minkowski inverse of a polytope does not exist. But the cancellation law holds, and this allows for the unique extension of the semigroup to the Grothendieck group: this is, by definition, the *group of virtual polytopes*. From a purely algebraic point of view, virtual polytopes are a most natural generalization of convex polytopes: in short, a virtual polytope is defined as a *formal Minkowski difference* of convex polytopes.

The first goal of this survey is to bridge the gap between this formal, algebraic definition and various interesting geometric interpretations (geometrizations). The second goal is to present different applications of the geometrization machinery, insights into the diverse questions that motivated the study of virtual polytopes, and to set up an appropriate framework for problems lying beyond this theory.

The main message that will emerge is that virtual polytopes retain many properties of convex polytopes, except convexity: a virtual polytope has a well-defined face lattice, support function, outer normal fan, volume, concept of enumeration of lattice points, and so on. However, the support function is no longer convex, the volume can be negative, the outer normal fan can contain non-convex cones, and so on.

It is not unusual in mathematics that different formalisms lead to essentially equivalent concepts: homology theories, (oriented) matroids, combinatorially rigid structures, abstract polytopes, and others have a multitude of crypto-morphic definitions, each with its own abstract structure and a set of axioms or consistency rules to be satisfied. Each is motivated by concepts arising in perhaps other areas of mathematics, and each time there are rules for converting from one formalism to another.

Virtual polytopes also fit this pattern. As generalizations of convex polytopes, they will be described as piecewise linear functions, collections of translated cones, invertible sheaves on a toric variety, and (in dimension three) stressed graphs on the unit sphere or (in dimension two) special types of two-dimensional polygonal chains.

However, in each setting we have one and the same group of virtual polytopes,<sup>1</sup> up to a canonical isomorphism.

Specifically, for each of the representations we describe a group of geometric objects which turns out to be canonically isomorphic to the group of virtual polytopes. Canonical isomorphisms between the various representations appear automatically: we go from one representation to the group of virtual polytopes, and from there to the other representation. However, in many situations direct isomorphisms appear naturally between some of these representations.

*Historical perspective.* The first systematic study of virtual polytopes, under this very name, appears in Khovanskii and Puklikhov's paper [1]. Their work was motivated by the algebraic geometry of toric varieties.<sup>2</sup> It was known that invertible sheaves on a projective toric variety form a group (the Picard group); it was also known that very ample sheaves correspond to convex polytopes (and form a semi-group), so the natural question arose: *what corresponds geometrically to the other elements of the Picard group?* Some technical details aside, the answer is: *The Picard group is isomorphic to the group of virtual polytopes.*

The idea of Minkowski subtraction of polytopes and convex sets can be traced back even further. In an early paper from 1939, A. D. Alexandrov [2] considered pointwise differences of support functions. Although not explicitly stated in his paper, this point of view leads to another way of defining virtual polytopes, which we describe in § 4.3.

Another important observation comes from the work of Groemer [3], who wrote the following in 1977: *It appears that an addition of non-convex sets... must necessarily take into account multiplicities of points, and this leads immediately to functions instead of ordinary sets.* And also: *It turns out that Minkowski addition is actually more akin to multiplication in a certain algebra than to addition.* We discuss this in § 4.1.

More recently and in a different context, Rodriguez and Rosenberg [4] introduced a class of polyhedral surfaces, called *polyhedral hedgehogs*,<sup>3</sup> which turn out to be a subclass of virtual polytopes. Subsequently, V. A. Alexandrov studied polyhedral hedgehogs in [5]. We present in § 5 a similar (but not identical) construction which covers the entire set of virtual polytopes. Martinez-Maure studied various aspects of hedgehogs and gave a sketch of an inductive definition (by dimension) of virtual polytopes in [6]. In § 5 we present an approach inspired, partially, by his ideas.

Virtual polytopes also appeared, implicitly, in McMullen's polytope algebra [7]; we expound on this subject in § 4.2.

*An important warning.* The theory of virtual polytopes is built upon an appropriate notion of *Minkowski subtraction*, but care must be exercised even with this most primitive ingredient. Indeed, various other definitions have appeared in the literature. For instance, the concept of Minkowski difference, as described in Schneider's book [8], is not the same as what we present in § 2. The problem is that Schneider's

---

<sup>1</sup>The precise definitions and further details appear in § 2.

<sup>2</sup>We present this as an application in § 6.5.

<sup>3</sup>In the original French, *hérissons*.

straightforward definition of Minkowski subtraction does not turn the semigroup of convex polytopes into a group: in his theory,  $P - P \neq 0$ .

*Overview of the survey.* We start in §2 with the basic definitions, and treat virtual polytopes as formal Minkowski differences. Important properties can already be defined in this setting.

The first non-trivial geometrization is described in §3 for two-dimensional virtual polytopes: we represent them as *coloured polygons*. This kind of ‘toy’ representation is very intuitive and gives a number of various examples but is possible only in dimension two.

Section 4 presents four types of geometrizations that work in all dimensions: 1) piecewise constant functions, which are elements of Khovanskii and Pukhlikov’s algebra; 2) elements of the first weight space of McMullen’s polytope algebra; 3) support functions; 4) systems of translated cones.

We return to dimension three in §5, where we present an approach based on rigidity theory. Here a virtual polytope appears as a system of springs in equilibrium on the sphere. A more intuitive representation is then given via what we call *Maxwell polytopes*, which are geometrizations of closed polyhedral surfaces whose faces are flat polygons; these faces, as well as the whole ‘surface’, may have self-intersections and exhibit other types of unusual features.

We conclude in §6 with several applications of virtual polytopes. We discuss here: 1) generalizations of A. D. Alexandrov-type problems for smooth convex bodies and convex polytopes; 2) volumes and mixed volumes of virtual polytopes; 3) Minkowski decompositions of polytopes; 4) the relationship to algebraic toric geometry.

## 2. Main definition

In this section we define virtual polytopes as formal Minkowski differences of convex polytopes and state some important properties that follow directly from the definition.

**2.1. Convex polytopes and Minkowski addition.** Throughout the paper, we assume that the ambient space for all our constructions is the Euclidean space  $\mathbb{R}^d$  with a fixed Cartesian coordinate system and the standard scalar product denoted by  $\langle x, y \rangle$ .

We identify the points of the space  $\mathbb{R}^d$  with their radius vectors, which enables us to speak of a sum of points.

Moreover, we often do not distinguish between affine subspaces and vector subspaces of  $\mathbb{R}^d$ . The point is that all our constructions are translation invariant, that is, do not depend on the choice of the origin.

*Convex polytopes.* A *convex polytope* is the convex hull of a non-empty finite point set in some space  $\mathbb{R}^d$ . When there is no risk of confusion, we may drop ‘convex’ and just write ‘polytope’. The set of all convex polytopes in  $\mathbb{R}^d$  is denoted by  $\mathcal{P}_d$ . To keep the notation simple, we omit the  $d$  and use  $\mathcal{P} := \mathcal{P}_d$ .

The *dimension* of a convex polytope  $K$  is the dimension of its *affine hull*, which is the minimal (with respect to inclusion) affine plane containing  $K$ . Thus, the

dimension of a convex polytope in  $\mathbb{R}^d$  is not necessarily  $d$ ; in particular, the polytope can be the degenerate zero-dimensional single-point polytope.

*Minkowski addition of convex polytopes.* From two convex polytopes  $K$  and  $L$ , the operation of Minkowski addition generates a new convex polytope  $K \otimes L$  defined by

$$K \otimes L = \{x + y \mid x \in K, y \in L\}$$

(an example in the plane is shown in Fig. 1).

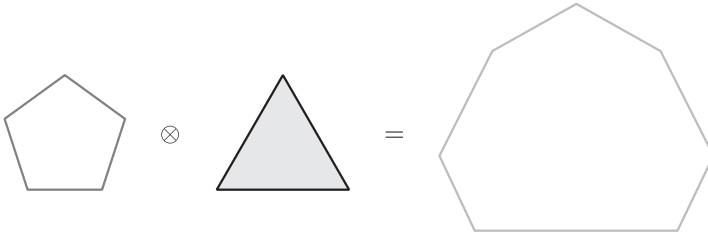


Figure 1. Minkowski sum of a pentagon and a triangle.

*A remark on notation.* Most of the literature on Minkowski addition uses the additive notation  $+$  or  $\oplus$ . However, it was recognized that in the context of the polytope algebra this operation behaves more like multiplication than addition. For this reason, various multiplicative symbols have come to be employed:  $\times$  in [3],  $*$  in [1], and  $\cdot$  in [7]. Here we adopt the multiplicative notation  $\otimes$ , in order to be consistent with its multiplicative role in the polytope algebra defined in § 4.1, and to emphasize its relationship with the tensor product of invertible sheaves described in § 6.5.

*Properties of the Minkowski sum.* The following basic properties lay the foundation for the theory surveyed in this paper.

1. The sum of a polytope  $K$  and a point  $p$  is the translation of the polytope  $K$  by the vector  $p$ , which we write as  $K + p$ .
2. The operation of Minkowski addition allows us to factor out translations. That is, for  $p_1$  and  $p_2$ , we have:

$$(K_1 + p_1) \otimes (K_2 + p_2) = (K_1 \otimes K_2) + (p_1 + p_2).$$

3. *Cancellation law:* if  $K \otimes L = K' \otimes L$  then  $K = K'$ .

With a few (explicitly stated) exceptions, we will **factor out translations**, that is, we will identify a polytope  $K$  and its translate  $K + p$ .

The operation of Minkowski addition turns the set  $\mathcal{P}$  of convex polytopes, factored by translations, into a commutative semigroup in which the above cancellation law holds. The *unit element*  $E$  is the convex polytope containing exactly one point. Since all such polytopes differ by a translation, we may assume that the unit element is represented by the origin:  $E = \{O\}$ .

**2.2. Virtual polytopes as the Grothendieck group.**

*Grothendieck group: general construction.* Whenever we have a commutative semi-group  $S$  (whose operation we denote multiplicatively) with a unit element  $e$ , it can be extended to a group if and only if it satisfies the cancellation law:

$$kl = ml \implies k = m.$$

The unique (up to isomorphism) minimal Abelian group containing  $S$  as a sub-semigroup is called the *Grothendieck group of  $S$* .<sup>4</sup> Its elements are equivalence classes of formal expressions (or *formal fractions*)  $kl^{-1}$  with  $k, l \in S$ , where  $k_1l_1^{-1}$  and  $k_2l_2^{-1}$  are identified whenever  $k_1l_2 = k_2l_1$ .

The embedding identifies each element  $k$  of the semigroup with the fraction  $ke^{-1}$ .

An elementary example of this construction is the group of non-zero rational numbers under multiplication, which extends the multiplicative semigroup of non-zero integers. Using this analogy, the convex polytopes will be our ‘integers’, while the virtual polytopes will correspond to the ‘rational numbers’.

**Definition 1.** The *group  $\mathcal{P}^*$  of virtual polytopes* is the Grothendieck group associated to the semigroup  $\mathcal{P}$  of convex polytopes under Minkowski addition.

The inverse in this group of a convex polytope  $K$  is denoted by  $K^{\otimes -1}$ . We can rephrase the definition as a combination of a few simple and useful properties:

- 1) a virtual polytope is a formal fraction  $K \otimes L^{\otimes -1}$ ;
- 2) two virtual polytopes represented by expressions  $K_1 \otimes L_1^{\otimes -1}$  and  $K_2 \otimes L_2^{\otimes -1}$  are identified whenever  $K_1 \otimes L_2 = K_2 \otimes L_1$ ;
- 3) the group operation literally repeats the rules of multiplication of two fractions, that is,

$$(K_1 \otimes L_1^{\otimes -1}) \otimes (K_2 \otimes L_2^{\otimes -1}) := (K_1 \otimes K_2) \otimes (L_1 \otimes L_2)^{\otimes -1};$$

- 4) the unit element is represented by  $E \otimes E^{\otimes -1}$ , where  $E$  is the unit element in  $\mathcal{P}$ , that is, the one-point polytope (the unit element may also be represented by any fraction of the form  $K \otimes K^{\otimes -1}$ ).

The natural inclusion

$$\mathcal{P} \hookrightarrow \mathcal{P}^*$$

of the group of convex polytopes in the group of virtual polytopes takes a convex polytope  $K \in \mathcal{P}$  to the formal fraction  $K_1 \otimes E^{\otimes -1}$ .

*Dimension of a virtual polytope.* Since a virtual polytope is not a set of points, the concept of dimension requires some care. We define the *dimension of a virtual polytope  $P$*  to be the smallest number  $k$  such that  $P$  can be expressed as  $P = K \otimes L^{\otimes -1}$ , with  $K$  and  $L$  convex polytopes lying in the same  $k$ -dimensional subspace of  $\mathbb{R}^d$ .

A remark is needed here: on the one hand, when speaking of convex (and virtual) polytopes we usually have in mind some fixed ambient space. On the other hand, each inclusion  $\mathbb{R}^d \subset \mathbb{R}^{d'}$  yields an inclusion  $\mathcal{P}_d \subset \mathcal{P}_{d'}$  which extends to all other

---

<sup>4</sup>The Grothendieck group is defined for any commutative semigroup. However, if the cancellation law does not hold, then the semigroup does not embed in its Grothendieck group.

constructions in this survey. In other words, if one is thinking not of the group as a whole but of a geometrization of a single virtual polytope or the sum (difference) of two polytopes, then one may not care about the ambient space.

Various geometric representations (*geometrizations*) of virtual polytopes are presented in subsequent sections. As a warm-up, we now discuss briefly the simplest cases, in dimensions zero and one.

*Virtual polytopes in dimension zero.* This is the trivial group with only one element (the unit element  $E$ ), which corresponds geometrically to the unique zero-dimensional polytope.

*Virtual polytopes in dimension one.* A convex polytope in  $\mathbb{R}^1$  is a segment. After factoring out the translations, we can identify a segment with a positive real number: its length. In this setting, the Minkowski addition of segments amounts to addition of positive real numbers. Thus, the semigroup  $\mathcal{P}$  of convex polytopes in  $\mathbb{R}^1$  is isomorphic to the semigroup  $\mathbb{R}_{\geq 0}$  of non-negative real numbers with the group operation  $+$ . The semigroup isomorphism maps a segment to its length. This implies that the group  $\mathcal{P}^*$  of virtual segments is isomorphic to  $\mathbb{R}$ .

For further reference, we state explicitly the three types of virtual segments:

- the segment of zero length, that is, a one-point polytope, representing the unit element  $E$ ;
- segments of positive length, that is, the usual convex segments;
- inverses (in the sense of Minkowski addition) of convex segments.

The inverses of convex segments may be thought of as having an associated negative sign, but a more intuitive convention makes use of colours instead of signs.

*Virtual polytopes in dimension one as coloured segments.* A simple visual representation of virtual segments is obtained by colouring regular segments: the convex segments (which correspond to positive numbers) are coloured in red. Their inverses (corresponding to negative numbers) are represented by convex segments coloured in blue. This way of visualizing virtual segments will be used in the next section for coloured stars and polygons, and it forms the basis for an inductive construction leading to virtual polytopes in higher dimensions.

We now formulate the Minkowski addition  $\otimes$  of virtual segments in terms of coloured segments:

- the sum of two segments of the same colour has length equal to the sum of the lengths of the summands, and it inherits the colour;
- two segments of different colours and equal length add up to the (uncoloured) one-point segment;
- two segments of different colours and unequal length add up to a segment whose colour is inherited from the longer of the two segments, and whose length is the difference of the two lengths (in particular, the inverse of a coloured segment is a segment of the same length but different colour).

**2.3. Facial structure of virtual polytopes.** Virtual polytopes, like the convex ones, have a well-defined facial structure. We start by reviewing a few important properties of faces of convex polytopes. Many of them carry over to virtual polytopes, except topology and convexity.

*Faces of convex polytopes.* Let  $K$  be a convex polytope in dimension  $d$ . For a given direction vector  $v \in \mathbb{R}^d$ , the *face  $K^v$  of  $K$  in the direction  $v$*  is the set of points  $p$  where the scalar product  $\langle v, \cdot \rangle$  attains its maximum value over all points  $p \in K$ . When  $v = 0$ , we get  $K^v = K$ . Otherwise,  $K^v$  is the intersection of  $K$  with the support hyperplane to  $K$  whose outward normal vector is  $v$ .

**Theorem 1.** *Faces of convex polytopes have the following properties [9].*

- Convexity of faces: *a face of a convex polytope is a convex polytope.*
- Being a face is a hereditary property: *a face of a face of a convex polytope  $K$  is itself a face of  $K$ .*
- Faces behave additively: *a face in the direction  $v$  of a Minkowski sum  $K \otimes L$  is the Minkowski sum of the faces in direction  $v$  of the summands:*

$$(K \otimes L)^v = K^v \otimes L^v.$$

The faces of a convex polytope, ordered by inclusion, form a partially ordered set called the *face lattice*. The face lattice captures the connectivities between faces of all dimensions, and contains information about the combinatorics and topology of the polytope.

We turn now to facial structure for virtual polytopes. Concrete examples and geometric interpretations are interspersed throughout the rest of the paper.

*Faces of virtual polytopes.* For a given direction vector  $v$ , we have a semigroup homomorphism  $K \rightarrow K^v$  taking convex polytopes in  $\mathbb{R}^n$  to convex polytopes lying in the corresponding hyperplane  $H^v$  with  $v$  as normal vector. In [10] it was shown that this map has a unique extension to a Grothendieck group homomorphism.

This enables us to define the *face of a virtual polytope  $P$  in the direction  $v$*  as the image  $P^v$  of  $K$  by this unique group homomorphism. As an immediate consequence, we have the following explicit formulation.

**Definition 2.** Let  $P = K \otimes L^{\otimes -1}$  be a virtual polytope, where  $K$  and  $L$  are convex polytopes, and let  $v$  be a direction vector. The face  $P^v$  is defined as

$$P^v = K^v \otimes (L^v)^{\otimes -1}.$$

This definition makes possible the following analogue of Theorem 1.

**Theorem 2.** *Faces of virtual polytopes have the following properties [10].*

- Faces are ‘virtual’: *a face of a virtual polytope is a virtual polytope.*
- Being a face is a hereditary property: *a face of a face of a virtual polytope  $P$  is itself a face of  $P$ .*
- Faces behave additively: *a face in the direction  $v$  of a Minkowski sum of two virtual polytopes is the Minkowski sum of the faces in direction  $v$  of the summands:  $(K \otimes L)^v = K^v \otimes L^v$ .*

The theorem lets us introduce in a natural way a partial order on the set of faces, where a face  $F$  of a virtual polytope  $P$  is *smaller* than a face  $F'$  of the same virtual polytope  $P$  if  $F$  is a face of  $F'$ .

The faces can be ranked by dimension. As usual, a  $k$ -dimensional face is referred to shortly as a *k-face*, 0-faces are called *vertices*, 1-faces are *edges*, and the  $(d - 1)$ -faces of a  $d$ -dimensional polytope are *facets*.

### 3. Virtual polytopes in dimension two

This section is devoted to the first non-trivial geometrization of virtual polytopes. This is not just a useful exercise to build up the intuition about what a virtual polytope might be, but it also covers the basic cases of an inductive construction that will be presented later in §5.

*Coloured stars.* A *coloured star* is a finite set of oriented segments in the plane such that:

- (a) one of the ends of each segment is the origin  $O$ ;
- (b) the segments are coloured in two colours (partitioned into two classes), red and blue;
- (c) each red segment is oriented in the direction away from the origin, whereas each blue segment is oriented towards the origin, thus giving us a collection of vectors;
- (d) the sum of these vectors equals zero;
- (e) no two segments intersect (except for the point  $O$ ).

A coloured star comes with a natural counterclockwise ordering on its segments.

*Star-to-polygon.* Taking the vectors of the star one by one according to the counterclockwise ordering and putting the tail of the next vector at the end of the previous one, we get an oriented polygon (oriented closed broken line) with coloured edges (see Fig. 3, for example).

By convention, the empty star yields a one-point polygon. (Nothing is coloured in this case because we only colour edges.)

*Coloured polygons.* A *polygon* is a cyclically ordered set  $P = \{p_1, \dots, p_n\}$  of points in the plane so that either  $n = 1$  or consecutive points  $p_i$  and  $p_{i+1}$  are distinct.<sup>5</sup> The cyclical ordering of the points means that we consider two polygons to be identical if one is obtained from the other by a renumbering corresponding to some power  $(2, 3, \dots, n, 1)^k$  of the cyclic permutation.

In other words, our polygons have an induced orientation, and the reverse orientation yields (in most cases considered in this paper) a different polygon. The consecutive points determine the edges of the polygon with non-zero length. We emphasize from the outset that we work here with arbitrary polygons, which may not be simple: they may self-intersect or have overlapping edges.

A *coloured polygon* is a polygon  $P = \{p_1, \dots, p_n\}$  with edges coloured red and blue which is obtained from some coloured star via the above ‘star-to-polygon’ procedure.

*Polygon-to-star.* Obviously, any coloured polygon uniquely restores a coloured star.

*Convex polytopes in dimension two, coloured polygons, and coloured stars.* The boundary of a convex polytope in dimension two is the polygon formed by its vertices and oriented counterclockwise. We colour the boundary polygon red, which gives us a coloured polygon. For convenience we sometimes refer to both the convex polytope in dimension two and its boundary as a convex polygon.

---

<sup>5</sup>Index arithmetic is done modulo  $n$  in the set  $\{1, 2, \dots, n\}$ .

We also consider limiting cases such as the *one-vertex polygon*  $\{p_1\}$  with no boundary edges, and the *segment-polygon*  $\{p_1, p_2\}$  with boundary consisting of two parallel (red) edges  $\overrightarrow{p_1 p_2}$  and  $\overrightarrow{p_2 p_1}$  with opposite orientations.

Using the star representation of a convex polygon, we compute a Minkowski sum by the following simple linear-time algorithm (illustrated in Fig. 2).

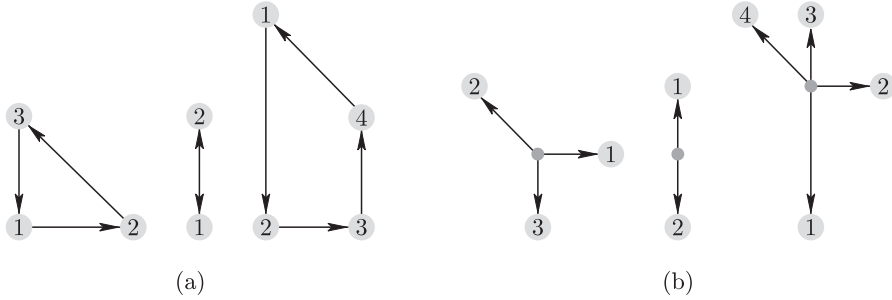


Figure 2. (a) The Minkowski sum of two convex polygons. (b) The sum of the corresponding stars.

**Algorithm** (computing the Minkowski sum of two convex polygons).

1. *Polygon-to-star*: convert the convex polygons into their convex stars.
2. *Geometric merge*: merge the two stars and then add the vectors with the same defining angle.
3. *Star-to-polygon*: reconstruct a new convex polygon from the resulting star.

With these concepts in place, we are now ready to introduce *virtual polygons*, that is, virtual polytopes in dimension two.

**3.1. The group of virtual polygons: geometric representations.** In this subsection we present a few concrete, geometric representations of virtual polygons: *coloured stars* and *coloured polygons* (see Fig. 3). In each case we also geometrize the operation of Minkowski addition (and subtraction).

*Convention about figures.* The colours of the edges are important in what follows. In order to distinguish them in black-and-white print, we mark blue edges by lines  $-\cdot-\cdot-\cdot-$ .

We have defined two sets (coloured stars and coloured polygons) together with the conversion rules. Our next step is to introduce group operations such that the conversion rules become group isomorphisms.

*Minkowski sum of coloured stars.* Given two coloured stars, their Minkowski sum (illustrated in Fig. 4) is a coloured star computed as follows.

1. Merge the stars.
2. If there are pairs of segments with the same defining angle (that is, two overlapping segments), then add them according to the one-dimensional rules and add the sum (an oriented segment with the same defining angle) to the list.
3. If the sum equals zero, eliminate the corresponding segments from the list.

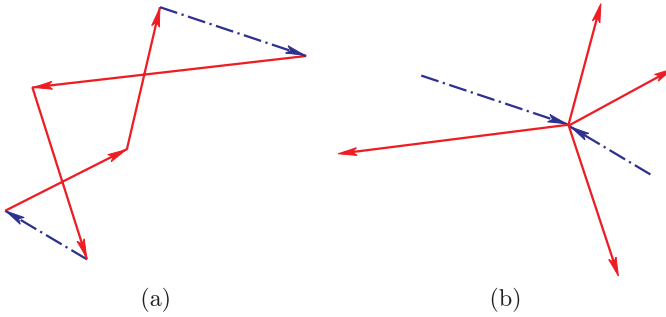


Figure 3. A virtual polygon represented as (a) a coloured polygon and (b) a coloured star.

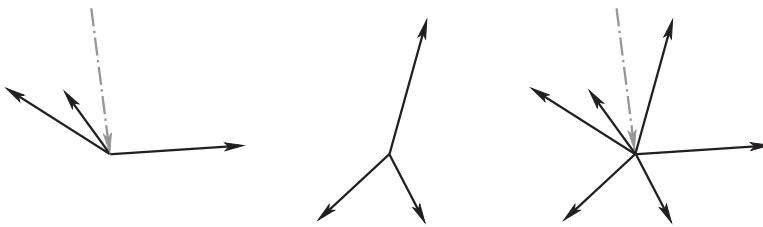


Figure 4. Minkowski sum of two virtual polygons, in the coloured star representation.

*Minkowski sum of coloured polygons.* Given two coloured polygons, their sum (see Fig. 5) is given by the following algorithm.

1. Take the coloured stars of the summands.
2. Add the coloured stars.
3. Retrieve a coloured polygon from the sum.

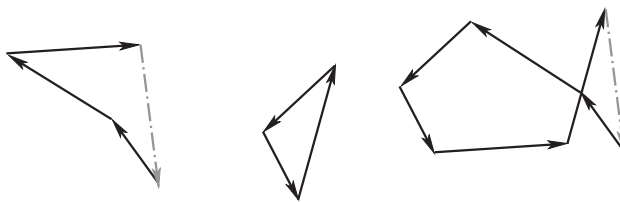


Figure 5. Minkowski sum of two virtual polygons, in the coloured polygon representation.

*Minkowski inverses.* The above operations turn the three sets of objects into groups, since all the elements are invertible (see Fig. 6):

- in the star representation, the inverse is obtained by reversing the colour and orientation of all star segments;

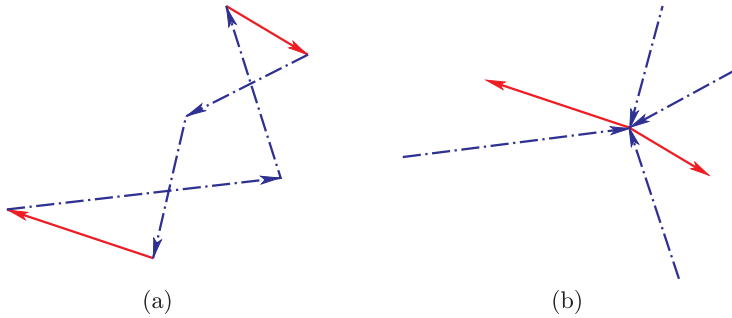


Figure 6. Minkowski inverse of the virtual polygon in Fig. 3 as (a) coloured polygon and (b) coloured star.

- the inverse of a virtual polygon is a rotation by  $\pi$  of the original polygon with reversed edge colours.

We summarize the previously described constructions as follows.

**Theorem 3.** *The groups of coloured polygons and coloured stars are isomorphic, and the isomorphism arises from the direct conversions described above (polygon-to-star and star-to-polygon). The two groups are canonically isomorphic to the group of virtual polytopes in dimension two.*

*Proof.* The semigroup of convex polytopes in dimension two embeds in each of the two groups, and each group is generated by the image of this inclusion.  $\square$

*Faces of a virtual polytope in dimension two represented by a coloured polygon.* A virtual polytope  $K$  in dimension two represented by a coloured polygonal chain  $(p_1, \dots, p_k)$  has three types of faces. The 0-faces are the points  $p_1, \dots, p_k$  and the (unique) 2-face is the polytope  $K$  itself. The 1-faces are coloured segments of two types, red and blue, as discussed in this section. Red edges represent 1-dimensional (convex) segments, whereas blue ones represent inverses to convex segments, as discussed in § 2.

**3.2. Examples of virtual polygons.** To help develop intuition, we now present a collection of illustrative examples.

**Example 1** (Minkowski inverse of a convex polygon). The inverse of a convex polygon is a rotation by  $\pi$  of the original polygon with all edges coloured blue.

**Example 2** (colourings of convex polygons). All of the 8 colourings of a triangle (of which 4 representatives are shown in Fig. 7) are virtual polygons. Only 4 of the colourings of a quadrilateral (see Fig. 8) are virtual polygons.

**Example 3** (six-gon and double-covered triangle). The double-covered triangle in Fig. 9 (on the right) is the degenerate case of the six-edge polygon on the left. Both arise by applying the star-to-polygon procedure to the coloured star shown. This illustrates the fact that virtual polygons, as opposed to convex polygons, may not

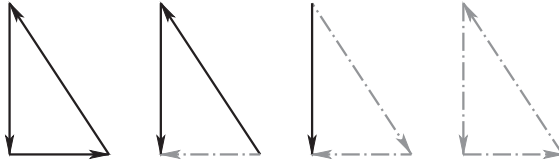


Figure 7. All 8 possible colourings of a triangle are virtual polygons (only 4 are shown).

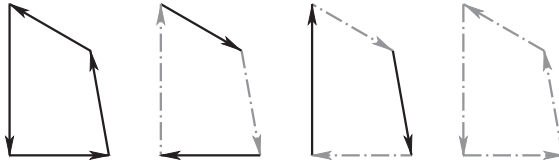


Figure 8. The 4 colourings of a quadrilateral which yield virtual polygons.

be simple. They may also have pairs of edges with parallel directions, but in the star these have to go in opposite directions.

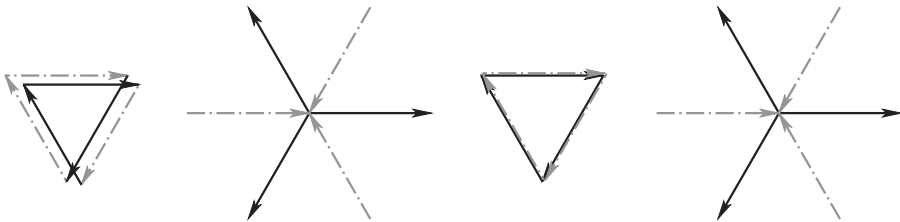


Figure 9. Left, a virtual 6-gon with parallel pairs of edges and its star. Right, an extreme situation where the 6-gon becomes a double-covered triangle.

**Example 4** (aligned edges). The two examples in Fig. 10 are virtual polygons with aligned edges. In Fig. 10 (left), the aligned edges have the same colour, and they must overlap in the polygon. In Fig. 10 (right), they have different colours, and are aligned but do not overlap in the polygon.

**Example 5** (multiple self-intersections). Virtual polygons can have multiple self-intersections, as illustrated in Fig. 11.

**3.3. Uncoloured virtual polygons.** We have so far described representations of virtual polytopes in dimension two as coloured polygons with some special properties. It is natural to ask whether one can forget the colours. In other words, is being ‘virtual’ just a property of the polygon (and not of the polygon with the extra colours on edges)? However, we show in this section that the colour-forgetting map from virtual polygons to uncoloured polygons is neither surjective nor injective.

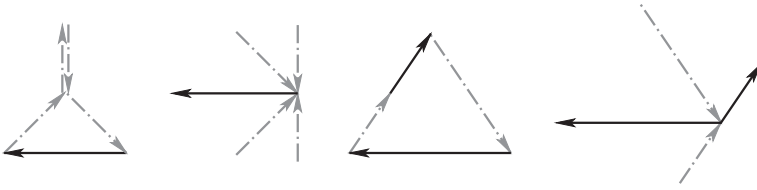


Figure 10. Left, alignment of two oppositely oriented edges with the same colour (shown slightly apart for clarity). Right, alignment of two similarly oriented edges with opposite colours.

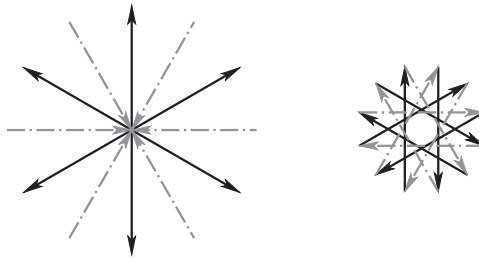


Figure 11. Minkowski difference of two regular hexagons.

**Definition 3.** A polygon with the property that it admits a colouring as a coloured polygon (that is, representing some virtual polytope) is called a *v-polygon*.

**Example 6** (not all polygons are *v-polygons*). The two examples in Fig. 12 are not *v-polygons*. In the first example the existence of groups of more than two parallel edges is an immediate indicator that this is not a virtual polygon, since no matter how we orient them, there will always be more than one edge vector with the same defining angle. For the second example, attempts to find a good colouring are unsuccessful: no colouring results in a star with segments arranged counterclockwise.

These examples raise the natural problem of *how to recognize polygons that have virtual polygon colourings*. An inefficient solution is to list all the  $2^n$  possible colourings on the edges and to keep only those that yield properly ordered coloured stars. However, we can show that there exists a simple linear-time algorithmic solution to this problem.

We have already seen in the examples in Fig. 7 and Fig. 8 that some polygons may have no good colouring that would make them virtual polygons, while others may have several.

*Remark.* The colourings of a *v-polygon* always come in pairs: if a colouring yields a virtual polytope  $K$ , then the inverse colouring yields the virtual polytope which is inverse to the centrally symmetric image of  $K$ .

**Definition 4** (ambiguous *v-polygon*). A *v-polygon* that admits more than three virtual polygon colourings will be called *ambiguous*.

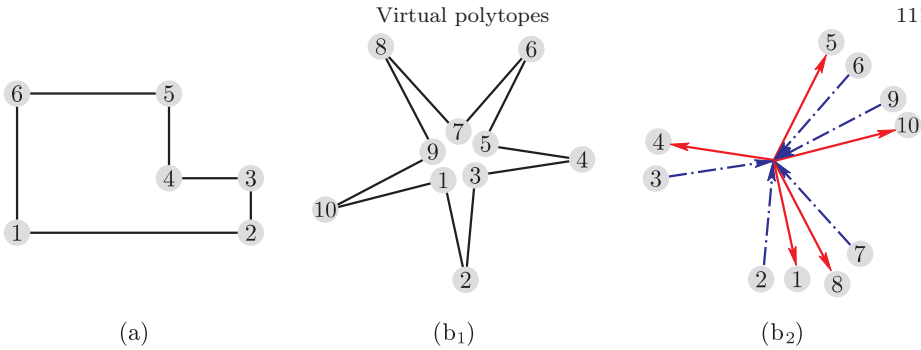


Figure 12. Two polygons which do not admit colourings as virtual polygons. (a) This polygon has more than two parallel edges. (b<sub>1</sub>) A polygon on which any attempt at producing a colouring would fail. (b<sub>2</sub>) For instance, a partial colouring of the first 8 edges inducing a counterclockwise ordering cannot be extended to a complete virtual polygon colouring.

**Example 7** (there exist ambiguous v-polygons). The triangle in Fig. 7 and the quadrilateral in Fig. 8 are ambiguous.

We conclude the section by stressing once again that the above geometrizations exist only in dimension two and do not generalize to higher dimensions.

#### 4. Virtual polytopes in arbitrary dimension

We turn now to four representations for virtual polytopes which are possible in all dimensions. For each one we describe a group of geometric objects which is shown to be canonically isomorphic to the group of virtual polytopes. Each section follows this pattern: (a) we first describe a set of geometrical objects together with a group operation; (b) we then show that the semigroup of convex polytopes embeds in this group; (c) finally, we show that the group is generated by the convex polytopes. Direct isomorphisms between pairs of these representations are also illustrated in some cases.

**4.1. The algebra of polytopal functions.** Virtual polytopes appear in the *algebra of polytopal functions* defined by Khovanskii and Pukhlikov [1], with motivations coming from the algebraic geometry of toric varieties. This last aspect will be discussed in § 6.5. To gain intuition, we compare virtual polytopes in dimension two represented by coloured polygons with the polytopal functions introduced in this subsection. We also note that this representation has a natural isomorphism with the combinatorial Picard group representation described later in § 4.4.

*Characteristic functions of convex polytopes.* We construct the algebra starting from the characteristic function  $I_K: \mathbb{R}^n \rightarrow \mathbb{R}$  of a convex polytope  $K$ , which is defined by

$$I_K(x) = \begin{cases} 1 & \text{if } x \in K, \\ 0 & \text{otherwise.} \end{cases}$$

*Polytopal functions.* A *polytopal function* is a function  $f: \mathbb{R}^n \rightarrow \mathbb{R}$  which is representable as a finite linear combination  $f = \sum \alpha_i I_{K_i}$  of characteristic functions of convex polytopes  $K_i$ . The coefficients  $\alpha_i$  (called *weights*) are arbitrary integers, possibly negative. The summands  $I_{K_i}$  may come from convex ‘pieces’ of different dimensions, including points.

We emphasize that in the construction of the algebra of polytopal functions *translations are not factored out*, that is, two polytopes that differ by a translation are considered to be different.

Such a representation of a polytopal function is never unique, as illustrated in Fig. 13. Here, the characteristic function of the larger rectangle is expressed as ‘rectangle plus rectangle minus segment’, or as ‘triangle plus triangle minus diagonal segment’.

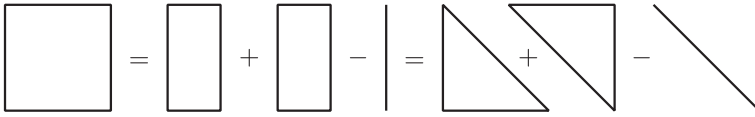


Figure 13. A polytopal function always has infinitely many decompositions.

*Ring structure.* The set of polytopal functions has a ring structure induced by the operation of *addition*, defined pointwise, and the operation of *multiplication*  $\otimes$ , which extends the Minkowski addition  $\otimes$  as follows.

*Multiplication of polytopal functions.* The product  $f \otimes g$  of two polytopal functions  $f = \sum_i \alpha_i I_{K_i}$  and  $g = \sum_j \beta_j I_{L_j}$  is defined as:

$$f \otimes g = \left( \sum_i \alpha_i I_{K_i} \right) \otimes \left( \sum_j \beta_j I_{L_j} \right) := \sum_{i,j} \alpha_i \beta_j I_{K_i \otimes L_j}. \tag{1}$$

The proof of correctness of this definition [1] (that is, that the definition does not depend on the particular representations of the summands) is based on an equivalent definition of the product of two polytopal functions  $f$  and  $g$  as the convolution with respect to the Euler characteristic  $\chi$ :

$$(f \otimes g)(x) = \int_{\mathbb{R}^n} f(x - y)g(y) d\chi(y).$$

Integration with respect to (and convolution against) the Euler characteristic is an elegant technique, first defined by Viro [11]. The idea of this notion is that the Euler characteristic  $\chi$ , being an additive function, in some sense resembles a measure. Therefore, in some particular cases one can integrate piecewise constant functions with respect to  $\chi$ . Since this technique will not be referred to again in our paper, we do not go into further details, which can be found in [11].

The two operations of addition and multiplication turn the set of polytopal functions into a commutative ring, with the identically-zero function as its zero element, and the characteristic function  $I_E$  as the unit element, where  $E = \{0\}$  is the one-point polytope containing the origin.

We focus in this paper on the ring structure, although the polytopal functions constitute an algebra over the rational numbers.

*Convex polytopes are invertible.* A remarkable property of the convex polytopes is that their characteristic functions are invertible in this ring.

We start with an auxiliary construction. Let  $K$  be a convex polytope. The interior of  $K$  taken in its affine hull is called its *relative interior* and is denoted by  $\text{Rint}(K)$ . The central symmetry with respect to the origin  $O$  is denoted by  $\text{Symm}$ .

It is not hard to show that the characteristic function of the relative interior of a convex polytope  $K$ , that is,

$$I_{\text{Rint}(K)}(x) = \begin{cases} 1 & \text{if } x \in \text{Rint}(K), \\ 0 & \text{otherwise,} \end{cases}$$

is a polytopal function.

**Theorem 4** ([1]). *For any convex polytope  $K$  its characteristic function  $I_K$  is invertible in the ring of polytopal functions. The inverse is expressed as*

$$(I_K)^{\otimes -1}(x) = (-1)^{\dim K} I_{\text{Rint}(\text{Symm } K)} = \begin{cases} (-1)^{\dim K} & \text{if } x \in \text{Rint}(\text{Symm } K), \\ 0 & \text{otherwise.} \end{cases}$$

**Corollary 5** ([1]). *The algebra of polytopal functions contains a multiplicative subgroup which, after factorization by translations, is isomorphic to the group of virtual polytopes. The canonical isomorphism maps each convex polytope  $K$  to its characteristic function  $I_K$ . In particular, the Minkowski inverse  $K^{\otimes -1}$  is mapped to the polytopal function described above in Theorem 4.*

This allows us to speak of *virtual polytopes represented by polytopal functions*. In the paper of Khovanskii and Pukhlikov [1] it is shown that virtual polytopes almost exhaust the class of all invertible polytopal functions.

**Theorem 6** ([1]). *Every invertible element of the ring of polytopal functions is, up to a sign, a virtual polytope. More precisely, for any invertible polytopal function  $f$ , either  $f$  or  $-f$  is a virtual polytope.*

A necessary and sufficient condition for a polytopal function to be invertible appeared in the same paper [1].

*Examples.* To build intuition, we give examples of virtual polytopes represented by polytopal functions in dimension two. Since such functions are piecewise constant, in the figures we mark the domains of constancy by the values of the function. Figure 14 depicts a function which is identically 1 strictly inside the triangle and identically zero outside the triangle and on its boundary. Figure 15 depicts a function which equals  $-2$  inside the triangle and  $-1$  on the boundary, and is zero outside.

Figure 16 illustrates multiplication of polytopal functions. The goal is to compute the Minkowski sum of the convex triangle and the open segment, with weight  $-1$ .

First we express the negatively weighted open segment as ‘*endpoint plus endpoint minus the (closed convex) segment*’. Next, we open the brackets and perform

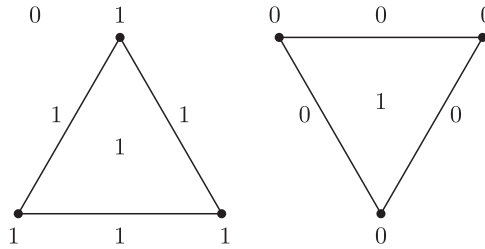


Figure 14. Left: polytopal function representing a convex triangle. Right: its inverse.

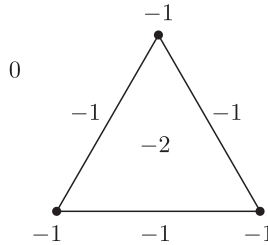


Figure 15. The double-covered virtual triangle (see Fig. 9), represented as a polytopal function.

classical Minkowski addition. This gives us two triangles and one trapezoid with weight  $-1$ . We depict them separately, but actually they overlap. Finally, one has to sum up the weights. This gives us the last figure.

As previously stated, the negatively weighted open segment is the Minkowski inverse of the convex segment. So the result of this computation is a virtual polytope, namely, the Minkowski difference of the triangle and the (convex) segment.

To compare the two representations for virtual polygons, Fig. 17 represents the virtual polygon in Fig. 3 by a polytopal function.

*Historical note.* The polytopal algebra was defined by Khovanskii and Pukhlikov in [1], although the basic ideas can be traced back to Groemer [3]. However, they used a different terminology (*convex chain*), which we have not adopted here because of possible confusion with other terminology we use. The alternative name of polytopal functions was used by Panina in [10] and [12].

We have confined ourselves to a description of the ring structure, and left the  $\mathbb{Q}$ -algebra structure beyond the scope of this article, referring the reader to [1].

**4.2. McMullen’s polytope algebra.** We turn now to a second representation for virtual polytopes, Peter McMullen’s polytope algebra  $\Pi$  [7]. It is closely related but not identical to the Khovanskii–Pukhlikov algebra of polytopal functions defined in the previous section. A crucial difference is that now the translations are factored out, and this has important algebraic consequences. In particular, it implies the existence of a lot of nilpotent elements, which in turn lead to a lot of invertible

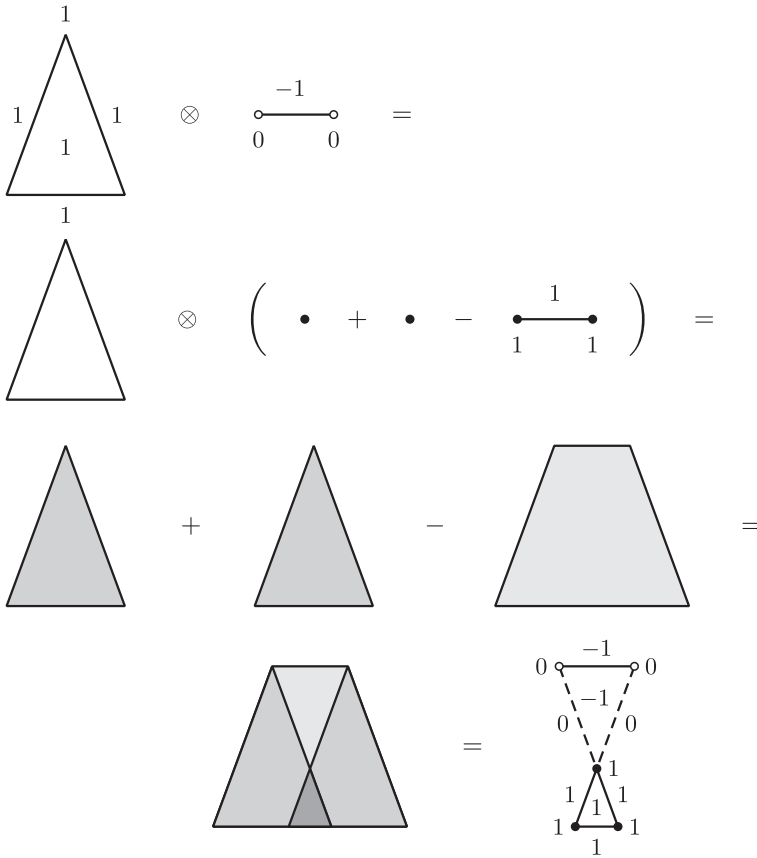


Figure 16. An example illustrating multiplication in the algebra of polytopal functions.

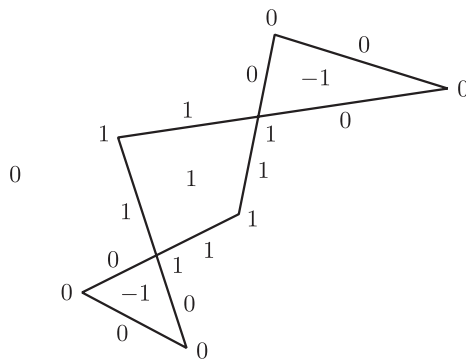


Figure 17. Virtual polygon in Fig. 3 represented as a polytopal function.

elements. By contrast, there are no nilpotent elements in the algebra of polytopal functions.

The group  $\mathcal{P}^*$  of virtual polytopes appears here in a completely different way, and now it is not isomorphic to the (multiplicative) group of invertible elements. As shown below,  $\mathcal{P}^*$  is isomorphic to an additive subgroup of the polytope algebra  $\Pi$  called the *first weight space*.

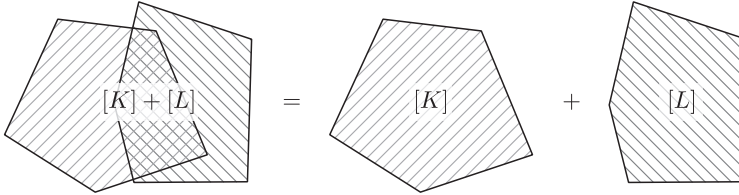


Figure 18. In McMullen’s algebra the polytopes are taken up to translation. Thus, these two objects are identified.

**Definition 5** (McMullen’s polytope algebra [7]). The polytope algebra  $(\Pi, +, \otimes)$  is defined over the set of symbols  $[K]$ , where  $K$  ranges over the set  $\mathcal{P}$  of all convex polytopes in  $\mathbb{R}^d$ . Additive expressions are subject to the equivalence relations

$$[K] + [L] = [K \cap L] + [K \cup L] \quad \text{if } K, L, K \cup L \in \mathcal{P}, \tag{2}$$

$$[K] = [K + t] \quad \text{if } K \in \mathcal{P} \text{ and } t \text{ is a translation vector.} \tag{3}$$

Multiplication is first defined for convex polytopes  $K$  and  $L$  via Minkowski addition  $[K] \otimes [L] := [K \otimes L]$ , and then extended by linearity to all elements of  $\Pi$ .

Thus, elements of the polytope algebra are linear combinations with integer coefficients of the form  $\sum \alpha_i [K_i]$ , subject to the equivalence relations (2) and (3). Figures 18 and 19 provide illustrations. The unit element  $E$  is the one-point polytope, and this is very similar to the algebra of polytopal functions.

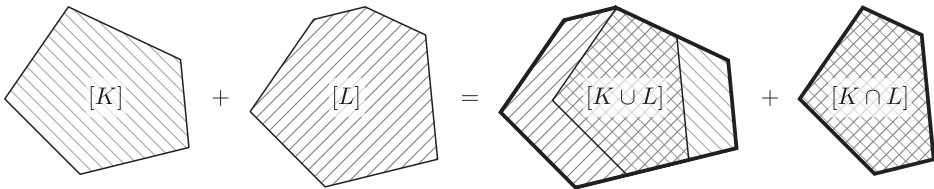


Figure 19. This illustrates the generating relations in McMullen’s algebra.

*Multiplication by rational numbers* in the polytope algebra is not always possible. But in the case when it is possible, it can be defined in a unique way. Here is the necessary and sufficient condition.

**Proposition 7** ([7]). *For any element  $\sum \alpha_i [K_i]$  of the polytope algebra and any non-zero integer  $a$  such that  $\sum \alpha_i$  is divisible by  $a$ , there exists a unique element  $f$  such that  $af = \sum \alpha_i [K_i]$  (so one can write  $f = \frac{1}{a} \sum \alpha_i [K_i]$ ).*

*If  $\sum \alpha_i$  is not divisible by  $a$ , then such an  $f$  does not exist.*

There exists a canonical surjective ring homomorphism from the algebra of polytopal functions to McMullen’s polytope algebra  $\Pi$  which makes the two algebras very similar. However, the group of units (invertible elements under multiplication) of the polytope algebra is much bigger than the group of virtual polytopes. The reason for this is that if  $\sum a_i = 0$ , then  $f = \sum a_i [K_i]$  is a nilpotent element, and therefore  $1 - f$  is invertible. The inverse  $(1 - f)^{-1} = 1 + f + f^2 + \dots$  is well defined, since the sum is finite in this case. Thus, an element  $\sum a_i [K_i]$  in McMullen’s polytope algebra is invertible if and only if  $\sum a_i = \pm 1$ .

*Weight spaces.* McMullen’s algebra  $\Pi$  has the structure of an (almost) graded algebra, that is, it is decomposable into a direct sum of graded components, called *weight spaces*. This decomposition has a deep interpretation in terms of the Chow rings associated to toric varieties, and will be briefly discussed in §6.5. Other details, although very interesting, are not relevant for our discussion and can be found in [7].

The decomposition of  $f$  into a sum of graded components is similar to the standard graded decomposition of the algebra of polynomials. The  $k$ th graded component of the algebra of polynomials consists of homogeneous polynomials of degree  $k$ . The latter can be recognized using dilation, since they are exactly those polynomials that satisfy  $p(\lambda x) \equiv \lambda^k p(x)$  for every real  $\lambda$ . Analogously, an element  $f$  in the polytope algebra is *homogeneous of degree one* if for every positive integer  $\lambda$  the dilation by  $\lambda$ , denoted by  $(\lambda)f$ , coincides with the sum of  $\lambda$  copies of  $f$ :

$$(\lambda)f = \underbrace{f + \dots + f}_{\lambda}.$$

It should be noted that a convex polytope is not homogeneous in this respect.

**Definition 6.** The first weight space of  $\Pi$  is defined as the set of homogeneous elements of degree one.

The first weight space is clearly an additive group.

**Example 8** (homogeneous element in dimension one). If  $K$  is a segment and  $P$  is a point, then  $[K] - [P]$  is homogeneous of degree one, and therefore belongs to the first weight space.

**Theorem 8** ([13], Lemma 2.2). *The group of virtual polytopes is isomorphic to the first weight space of McMullen’s polytope algebra.*

*The isomorphism sends a convex polytope  $K$  to*

$$\log K = \sum_{i=0}^{\infty} (-1)^{i+1} \frac{([K] - E)^i}{i},$$

where  $E$  is the one-point polytope, that is, the unit element in  $\Pi$ .

Since  $[K] - E$  is a nilpotent element, the above sum is finite.

It will be seen in §6.5 that this theorem relates the Picard group of a toric variety to the group of virtual polytopes.

*Historical note.* The definition of the polytope algebra was motivated by the *scissors congruence problem*, which in turn originated from Hilbert's Third Problem. The group of all (isometric) motions of the space used in the classical setting is replaced here by translations. The algebra can be viewed as the universal group for translation-invariant finitely additive measures on convex polytopes (such measures are called *translation-invariant valuations*).

The polytope algebra has several remarkable isomorphic interpretations. One is the direct limit of Chow rings of toric varieties [14], and another is via piecewise polynomial functions with respect to some fan [15].

The most remarkable thing about McMullen's algebra is its relationship to the *g-theorem* that characterizes the numbers of faces of simple polytopes. Necessary and sufficient conditions were conjectured in 1970 by McMullen. The first proof of the necessity part by Stanley [16] used an approach from algebraic geometry. Later on, other necessity proofs were given: a purely combinatorial one was due to Stanley, while McMullen [17] proved the necessity part using the weight space decomposition in the polytope algebra. We also mention here the proof by Timorin (see [18]).

Convex polytopes yield another interesting algebraic structure, the *ring of simple polytopes* (see [19] and [20]). However, that does not contain the group of virtual polytopes.

**4.3. Support functions.** The support function of a convex body represents a well-established concept in convex geometry. Since it behaves additively with respect to Minkowski addition, the subtraction of support functions is expected to correspond to Minkowski difference.

We show that just like convex polytopes, virtual polytopes have well-defined piecewise linear support functions, and therefore outer normal fans. Although the convexity property of the support function and of the fan is relaxed, all the other properties are maintained.

*Cones, fans, and spherical fans.* A cone  $\sigma \subset \mathbb{R}^n$  is a closed set of points preserved by homotheties with centre at the origin: for any  $x \in \sigma$  and any non-negative  $\lambda$ , the point  $\lambda x$  lies in  $\sigma$ . Most publications on convex polytopes (for instance, [9]) assume that a cone is convex, since this is the case in the context of convex polytope theory. For our purposes, we will have to drop this assumption, hence our cones may not be convex.

We work with *polyhedral cones*, that is, those having a piecewise linear boundary. The ambient space  $\mathbb{R}^n$  and the set containing just the origin  $\{O\}$  are special cases of cones. A fan  $\Sigma$  is a finite collection of polyhedral cones in  $\mathbb{R}^n$  such that: (a) any face of a cone  $\sigma \in \Sigma$  belongs to  $\Sigma$ ; (b) for any two cones  $\sigma_1, \sigma_2 \in \Sigma$ , the intersection  $\sigma_1 \cap \sigma_2$  is a union of faces of both  $\sigma_1$  and  $\sigma_2$ ; (c) the union of all the cones equals  $\mathbb{R}^n$ . A *convex fan* consists only of convex cones.

For a more intuitive visualization, we also introduce a *spherical fan*, which is the intersection of the (standard unit) sphere with a fan. This yields a tiling of the sphere into spherical polytopes (which may be non-convex). Each spherical fan extends to a fan, so we have an easy direct correspondence between these concepts.

A fan  $\Sigma$  is said to be *coarser* than a fan  $\Sigma'$ , or equivalently,  $\Sigma'$  is called a *refinement* of  $\Sigma$ , if  $\sigma \in \Sigma'$  implies that there exists a cone  $\tau \in \Sigma$  such that  $\sigma \subseteq \tau$ . An example is given in Fig. 20.

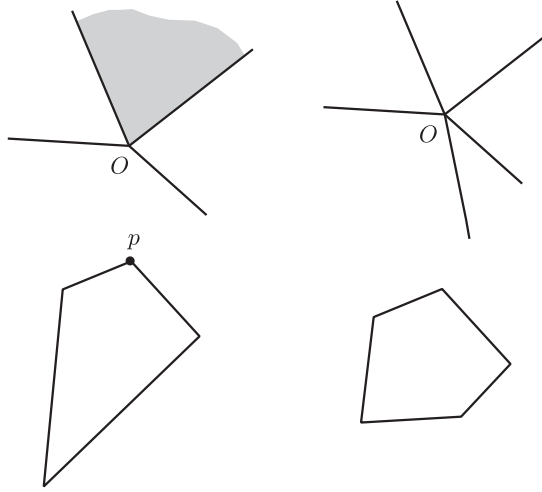


Figure 20. Two convex polygons together with their outer normal fans.

The *support function* of a convex polytope  $K$  is the function

$$h_K: \mathbb{R}^n \rightarrow \mathbb{R},$$

defined by

$$h_K(x) = \max_{y \in K} \langle x, y \rangle,$$

where  $\langle x, y \rangle$  is the standard scalar product.

For a generic  $x$  the maximum of the scalar product  $\langle x, \cdot \rangle$  is always achieved at one of the vertices of the polytope. For the example in Fig. 20, if  $x$  lies in the shadowed cone, then the maximum is attained at the vertex  $p$ . Consequently, on the shadowed cone the support function of the polygon coincides with the support function of the point  $p$ , which is the linear function  $\langle p, x \rangle$ . Figure 21 gives an example.

A few well-known properties of the support functions of convex polytopes are summarized in the following lemma.

**Lemma 9.** *Let  $K$  and  $L$  be convex polytopes. Let  $K + t$  be the translation of  $K$  by a vector  $t$ . Then:*

- 1)  $h_K$  is a convex piecewise linear function;
- 2) the support functions  $h_K$  and  $h_{K+t}$  differ by a linear summand;
- 3)  $h_K$  is positively homogeneous, that is,  $h_K(\lambda x) = \lambda h_K(x)$  for  $\lambda \geq 0$ , and in particular,  $h_K$  equals zero at the origin  $O$ ;
- 4) the support function of a Minkowski sum equals the sum of the support functions, that is,

$$h_{K \otimes L} = h_K + h_L.$$

*Outer normal fan of a convex polytope.* There are two equivalent ways to define the fan of a convex polytope. We shall use the second definition below of the fan of a virtual polytope.

- For a convex polytope  $K$ , the linearity domains of its support function  $h_K$  yield a fan  $\Sigma_K$  called the *outer normal fan of the polytope  $K$* , or simply the *fan of the polytope  $K$*  for short.
- Alternatively, the fan of a convex polytope can be defined as follows. For each face  $F$  of  $K$ , define a cone

$$\sigma_F := \{v \in \mathbb{R}^n : K^v = F\}$$

consisting of those vectors  $v$  such that the face  $K^v$  equals  $F$ . The fan of  $K$  is the set of all the closures of all such cones when  $F$  ranges over all the proper faces of  $K$ .

An example is illustrated in Fig. 20.

The definition immediately implies the following duality property.

**Lemma 10.** *The faces of a convex polytope  $K$  are in a bijective correspondence with the cones of the fan  $\Sigma_K$ . Furthermore:*

- 1) *a  $k$ -dimensional face of  $K$  corresponds to an  $(n-k)$ -dimensional cone of  $\Sigma_K$ ;*
- 2) *the affine hull of a face and the affine hull of the corresponding cone are orthogonal;*
- 3) *this correspondence reverses inclusion.*

**Example 9.** Figure 21 depicts a pentagon, its fan, and the graph of the support function.

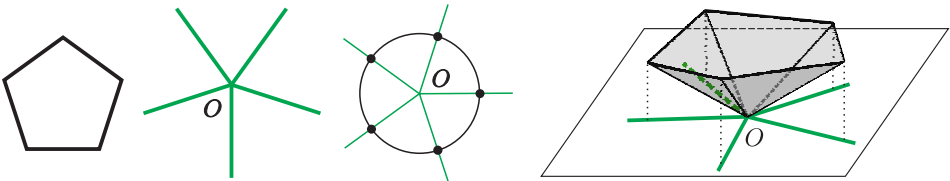


Figure 21. A convex pentagon, its outer normal fan, its spherical fan, and the graph of its support function.

*The group of support functions.* We consider now the set of all convex continuous positively homogeneous piecewise linear functions defined on  $\mathbb{R}^n$ . Each of them is the support function of some uniquely defined convex polytope. With pointwise addition, this set forms a semigroup. We denote by  $\mathcal{S}$  this semigroup factored by globally linear functions. The map taking each polytope  $K$  to its support function  $h_K$  establishes an isomorphism between the semigroup  $\mathcal{P}$  of convex polytopes modulo translations and the semigroup  $\mathcal{S}$ .

We extend the semigroup  $\mathcal{S}$  to the *group of support functions*, that is, the Grothendieck group associated to it. It consists of all continuous positively homogeneous piecewise linear functions  $h$  defined on  $\mathbb{R}^n$ , modulo globally linear functions.

Passing to the Grothendieck group means that we allow subtraction of functions. Consequently, we lose convexity, but all the other properties in Lemma 9 are preserved.

The following definition describes the canonical isomorphism between the group of virtual polytopes and the group of support functions.

**Definition 7.** Let  $K = L \oplus M^{\otimes -1}$  be a virtual polytope. Let  $h_L$  and  $h_M$  be the support functions of  $L$  and  $M$ , respectively. The *support function* of  $K$  is defined as  $h_K := h_L - h_M$ .

Since the group of support functions is generated by convex functions, we have the following theorem.

**Theorem 11.** *The group of virtual polytopes and the group of support functions are canonically isomorphic. The isomorphism sends a virtual polytope to its support function.*

**Definition 8.** Given a virtual polytope  $K$ , each face  $F$  of  $K$  yields a cone

$$\sigma_F := \{v \in \mathbb{R}^n : K^v = F\}$$

consisting of those vectors  $v$  such that the face  $K^v$  equals  $F$ . The collection of closures of all such cones when  $F$  ranges over all proper faces of  $K$  is called the fan of the virtual polytope  $K$ .

In contrast to the convex case, the cones of the fan are not necessarily convex (see Figs. 22 and 23).

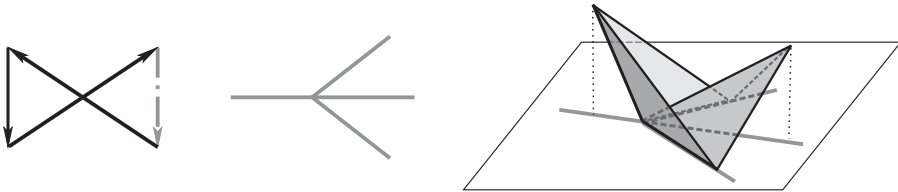


Figure 22. Left: a virtual polytope represented by a coloured polygon. Middle: its fan. Right: the graph of its support function. In this particular case the fan is convex, but the support function is not convex.

Given a virtual polytope  $K$ , the cones of maximal dimension of the fan correspond to vertices of  $K$ . This yields a simple, yet important lemma.

**Lemma 12.** *A virtual polytope  $K$  is uniquely determined by its fan, vertex set, and the (duality) map between the vertices of  $K$  and the cones of  $\Sigma_K$  of maximal dimension.*

*Proof.* Indeed, we retrieve the support function  $h_K(x)$  as the piecewise linear function whose restriction to each of the maximal cones  $\sigma_i$  equals the scalar product  $(p_i, x)$ , where  $p_i$  is the vertex corresponding to the cone  $\sigma_i$ .  $\square$

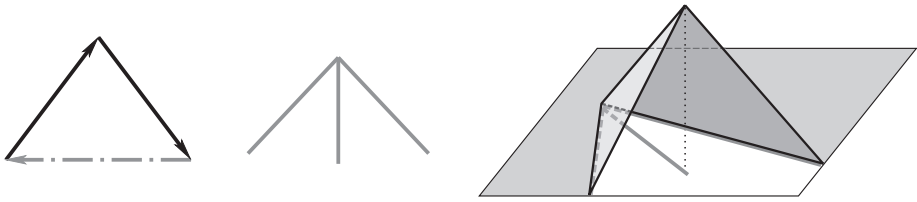


Figure 23. Left: a virtual polytope represented by a coloured polygon. Middle: its fan. Right: the graph of its support function. In this particular case, both the fan and its support function are not convex.

**Example 10.** In dimension two the fan is obtained from the coloured star representation by rotating clockwise through the angle  $\pi/2$  and by forgetting the colours. After the rotation, each (coloured) segment gives a ray (its colour does not matter).

We conclude with a list of virtual triangles, shown in Fig. 24 simultaneously as polytopal functions and as coloured chains, together with their fans.

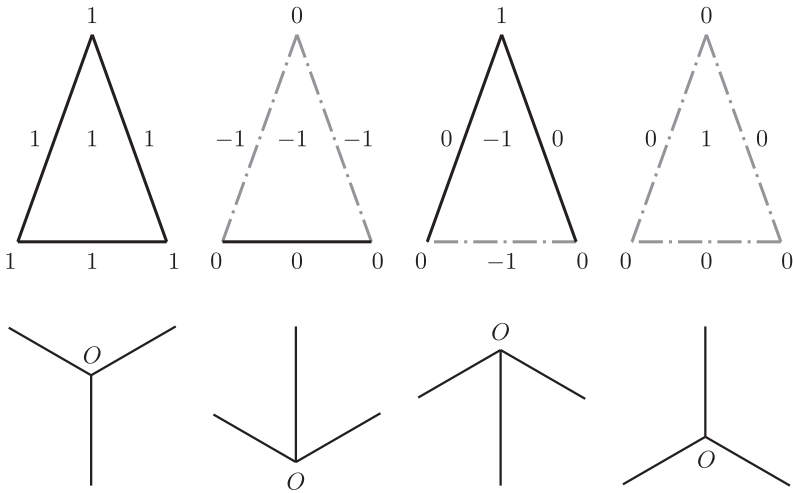


Figure 24. Virtual triangles represented as polytopal functions and as coloured polygons, together with their fans.

*Historical notes.* The idea of subtracting support functions of convex bodies pointwise can be traced back to several sources in the mathematical literature, and hence this representation of virtual polytopes may not be a completely new concept. We mention in particular an early paper [2] from 1939 by A. D. Alexandrov, who considered pointwise differences of support functions when proving a theorem giving a characterization of the sphere. This theorem is the starting point for Alexandrov’s problem discussed in § 6.1. However, this terminology (the support function of a virtual polytope) has appeared only recently: the first systematic and explicit study of virtual polytopes defined via their support functions was carried out in [1]

(see also [21]). Fans of virtual polytopes appeared (only for 3D) in [4] by Rodriguez and Rosenberg and in [5] by V. Alexandrov, but these authors considered only a restricted class of virtual polytopes called *polyhedral hedgehogs*, which are virtual polytopes with convex fans. As we have seen, these do not cover the entire group of virtual polytopes. Support functions and fans of virtual polytopes were also used by Panina in [10], [22]–[24].

**4.4. The combinatorial Picard group: systems of translated cones.** In this section we describe a representation for general virtual polytopes by *systems of translated cones*, a term due to Ewald [9]. There exists a direct correspondence between this representation and the representation in § 4.1 by polytopal functions.

*Dual cone.* In this section all cones are convex. This condition is necessary for the correct definition of a dual cone. Given a convex cone  $\sigma$ , its *dual cone*  $\check{\sigma}$  is defined by

$$\check{\sigma} = \{x \in \mathbb{R}^n : \langle x, y \rangle \leq 0 \text{ for all } y \in \sigma\}.$$

*Translated cones for a convex polytope.* Let  $K$  be a convex polytope and  $\Sigma$  its fan. Let a cone  $\sigma \in \Sigma$  correspond by duality to a vertex  $p_\sigma$  of  $K$ . Then the cone spanned by  $K$  at the vertex  $p_\sigma$  is the translate by  $p_\sigma$  of the dual cone  $\check{\sigma}$ . In other words, it equals the Minkowski sum  $p_\sigma \otimes \check{\sigma}$ .

Analogously, if a cone  $\sigma \in \Sigma$  corresponds by duality to a face  $F$  of  $K$ , then the cone spanned by  $K$  at the face  $F$  is a translate of the cone  $\check{\sigma}$  by some vector  $p_\sigma$ , where  $p_\sigma$  can be chosen to be any point in the affine hull of  $F$ .

A convex polytope thus naturally yields a system of translated cones. This is illustrated in Fig. 25 and Fig. 27.

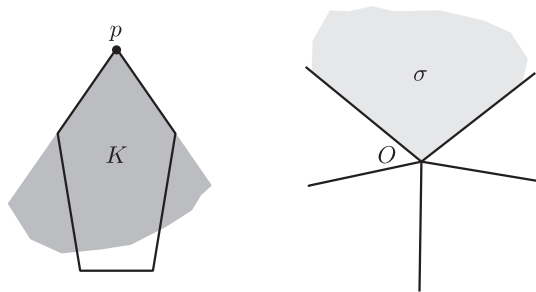


Figure 25. Left: a cone  $\sigma$  of the fan corresponding to the vertex  $p_\sigma$  of the polygon  $K$ . Right: the translated cone  $p_\sigma \otimes \check{\sigma}$ .

The following *Brianchon–Gram decomposition* [25] (also known as the Gram–Sommerville formula, or Gram’s equation) is classical (see Fig. 26).

**Theorem 13** ([25]). *For a convex polytope  $K$  and the associated system*

$$\{p_\sigma \otimes \check{\sigma}\}_{\sigma \in \Sigma}$$

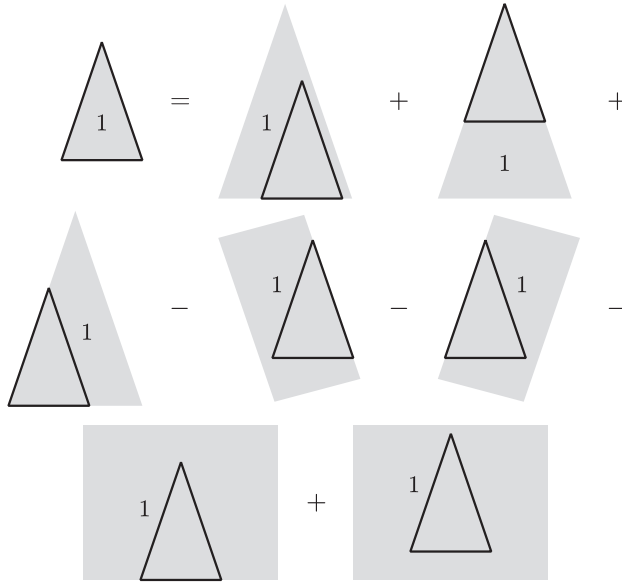


Figure 26. Brianchon–Gram decomposition of a convex triangle.

of translated cones, the characteristic function of  $K$  decomposes into the alternating sum of the characteristic functions of the cones:

$$I_K = \sum_{\sigma \in \Sigma} (-1)^{\text{codim } \sigma} I_{p_\sigma \otimes \check{\sigma}}.$$

The following orthogonality property follows directly from Lemma 10.

**Lemma 14.** For every cone  $\sigma \in \Sigma$  and every one of its faces  $\tau$ , the vector  $p_\sigma - p_\tau$  is orthogonal to the affine span  $\text{aff}(\tau)$ .

*Systems of translated cones.* The above discussion suggests the following definition.

**Definition 9.** Let  $\Sigma$  be a convex fan in  $\mathbb{R}^n$  and let  $\{p_\sigma \in \mathbb{R}^n : \sigma \in \Sigma\}$  be the collection of translation vectors associated to its cones. The collection

$$\{p_\sigma \otimes \check{\sigma}\}_{\sigma \in \Sigma}$$

of translated dual cones is called a system of translated cones with respect to the fan  $\Sigma$  if the following (consistency) condition holds: for every cone  $\sigma \in \Sigma$  and every one of its faces  $\tau$ , the vector  $p_\sigma - p_\tau$  is orthogonal to the affine span  $\text{aff}(\tau)$ .

*Remark.* This definition differs somewhat from Ewald’s in [9] in that we do not assume that the fan involved is rational, and we do not require that the polytopes involved are lattice polytopes (that is, have integer coordinates of the vertices). These conditions necessarily appear later, when we pass to toric varieties. But we stress that it is necessary for the fan to be convex, since otherwise duality is not well defined.

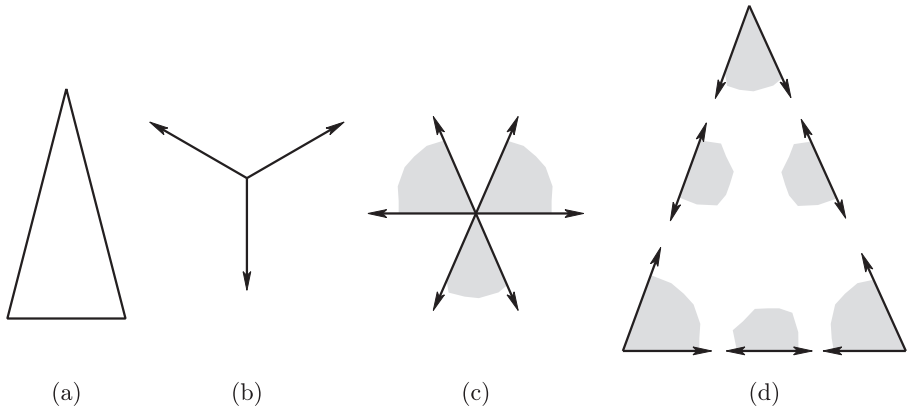


Figure 27. (a) A triangle. (b) Its fan. (c) Cones dual to the cones of the fan. (d) Translated dual cones.

*Group structure on systems of translated cones.* Assuming that a fan  $\Sigma$  is fixed, we now endow the system of translated cones with a group structure. The group operation is defined by

$$\{p_\sigma \otimes \check{\sigma}\}_{\sigma \in \Sigma} + \{p'_\sigma \otimes \check{\sigma}\}_{\sigma \in \Sigma} = \{(p_\sigma + p'_\sigma) \otimes \check{\sigma}\}_{\sigma \in \Sigma}.$$

We get a commutative group with zero element  $\{O \otimes \check{\sigma}\}_{\sigma \in \Sigma}$ .

To factor out (global) translations, we factorize in the above group by elements of the form  $\{p \otimes \check{\sigma}\}_{\sigma \in \Sigma}$ . After the factorization we get a group  $\mathcal{C}\mathcal{P}_\Sigma$  which is called (in Ewald’s book [9]) the *combinatorial Picard group related to the fan  $\Sigma$* .

*The group of virtual polytopes related to a fan.* We are now ready to relate systems of translated cones to virtual polytopes. The *group  $\mathcal{P}_\Sigma^*$  of virtual polytopes related to a fan  $\Sigma$*  is the subgroup of  $\mathcal{P}^*$  consisting of those elements whose support function is linear on each of the cones in  $\Sigma$ . Equivalently, a virtual polytope  $K$  is related to the fan  $\Sigma$  if its fan  $\Sigma_K$  is coarser than  $\Sigma$ .

The following theorem establishes the canonical isomorphism between the combinatorial Picard group  $\mathcal{C}\mathcal{P}_\Sigma$  and the subgroup of virtual polytopes defined above.

**Theorem 15.** *The combinatorial Picard group  $\mathcal{C}\mathcal{P}_\Sigma$  is isomorphic to the subgroup of virtual polytopes related to the fan  $\Sigma$ . The isomorphism sends a convex polytope to the associated system of translated cones. Once defined for convex polytopes, the isomorphism extends to all virtual polytopes.*

**Example 11.** Figure 28 illustrates two systems of translated cones for a convex triangle and its inverse. The fan of a convex triangle contains 7 cones: three two-dimensional cones, three one-dimensional cones (rays), and the one-point cone  $\{O\}$ . Consequently, the dual cones are three pointed cones, three half-planes, and the entire plane (which is dual to  $\{O\}$ ). Figure 27 shows all of them, whereas Fig. 28 shows only the pointed dual cones.

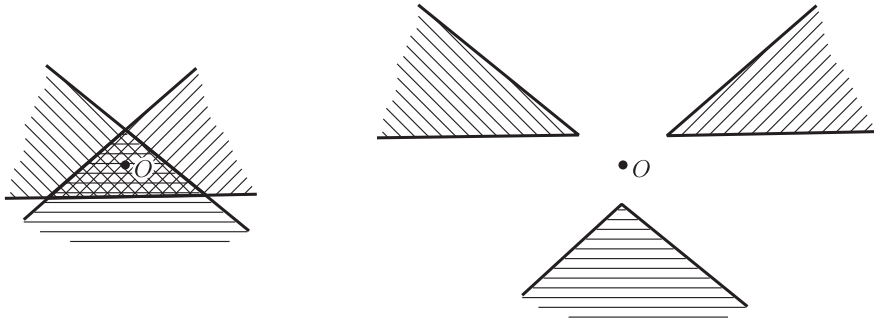


Figure 28. Systems of translated cones for a triangle and its inverse.

From subgroups of virtual polytopes related to a particular fan, we now extend the definition to the entire group of virtual polytopes. Given a fan  $\Sigma$  and a refinement  $\Sigma'$  of it, we have a natural inclusion  $\mathcal{P}_\Sigma^* \rightarrow \mathcal{P}_{\Sigma'}^*$ . This allows us to speak of the *inductive limit* of the groups  $\mathcal{P}_\Sigma^*$ , which means that we take the union of all such groups and identify elements by using the indicated inclusions. We arrive at the following theorem.

**Theorem 16.** *The group  $\mathcal{P}^*$  of virtual polytopes is isomorphic to the inductive limit of the groups  $\mathcal{C}\mathcal{P}_\Sigma$ .*

For a virtual polytope given by a system of translated cones there is an elegant way to represent it as a polytopal function by using a direct generalization of the aforementioned Brianchon–Gram decomposition for convex polytopes.

**Theorem 17** ([1]). *For a virtual polytope given by a system of translated cones, that is,*

$$K = \{p_\sigma \otimes \check{\sigma}\}_{\sigma \in \Sigma},$$

*its canonical image in the algebra of polytopal functions is the function*

$$\sum_{\sigma \in \Sigma} (-1)^{\text{codim } \sigma} I_{p_\sigma \otimes \check{\sigma}}.$$

As an example, this formula can be checked for a triangle using Fig. 27.

*Remark.* Analogous constructions are valid if we restrict ourselves to *lattice polytopes*, that is, polytopes whose vertices lie in the standard lattice  $\mathbb{Z}^n \subset \mathbb{R}^n$ . In this case we obtain the *group  $\mathcal{P}_\mathbb{Z}^*$  of lattice virtual polytopes*, the *group  $\mathcal{P}_{\mathbb{Z}, \Sigma}^*$  of lattice virtual polytopes related to a fan*, the *combinatorial lattice Picard group  $\mathcal{C}\mathcal{P}_\Sigma^\mathbb{Z}$* , and also the group  $\mathcal{C}\mathcal{P}_\Sigma$ . In this framework it makes sense to consider only rational fans.

To summarize, we have described another equivalent representation of virtual polytopes. This turns out to be the most suitable representation for working with toric varieties (see § 6.5), since a system of translated cones immediately yields an invertible sheaf on a toric variety.

*Historical note.* The name ‘Picard group’ clearly indicates the original motivation of Pukhlikov and Khovanskii in connection with the Picard group of a toric variety. It should be mentioned that the Picard group of a projective toric variety has several equivalent representations: as the group of invertible sheaves, as the group of divisors, and as the group of line bundles. For a toric variety the translated cones give yet another representation originating in convex geometry.

## 5. Virtual polytopes in dimension three

In this section we give two representations of virtual polytopes which are specific to dimension three. In a sense they generalize the case of dimension two, where virtual polytopes appeared as coloured polygons. Therefore, one would expect some kind of polyhedral surface. The first approach represents virtual polytopes as *stressed non-crossing graphs on the sphere*. Simple rules turn the set of spherical stressed graphs into a group, which is shown to be isomorphic to the group of virtual polytopes. The second representation is as a subfamily of *Maxwell polytopes*, so called because these types of polyhedral surfaces appeared for the first time in the work of James C. Maxwell. Both geometrizations of 3D virtual polytopes in this section are inspired by, and intimately related to, Maxwell’s theory [26] of planar stressed non-crossing graphs and polyhedral liftings.

Diverse concepts of polytopes appear in the literature: some are non-convex, some have non-convex faces, some may have a non-spherical topology, and so on. But the polytopes that we introduce here diverge even further from these familiar examples. In our setting, Maxwell polytopes still have vertices, edges, and faces. The faces are flat polygons, but they need not be simple, that is, they may self-intersect.

### 5.1. Virtual polytopes as spherical stressed graphs.

*Non-crossing spherical graphs.* A graph is a pair  $G = (V, E)$ , with a finite set  $V = \{1, 2, \dots, n\}$  of vertices and a finite set  $E$  of edges. We allow loops and parallel edges. We also include the *single-loop graph*, which is one closed edge with no vertices on it. A graph may contain the single-loop graph as a connected component. For technical reasons that will become clear later, we also assume that there are no isolated vertices and no vertices of degree 2.

A *spherical realization* (or *placement*) of the graph is an injective map

$$p: V \rightarrow S^2$$

of its vertices to the unit sphere  $S^2$ , together with a function that maps edges to geodesic segments (great-circle arcs) on the sphere. An edge with endpoints  $i$  and  $j$  is mapped to a geodesic segment with endpoints at  $p_i$  and  $p_j$ . The placement is said to be non-crossing or an embedding if the edge segments do not cross and do not overlap. The edges are not necessarily mapped to shortest geodesics, so if the vertices of an edge are fixed, then there are (at least) two ways to place the connecting edge. We also assume that the single-loop graph embeds as a great circle (with no vertices).

Such a spherical realization induces a *facial structure* on the graph. The faces are the connected components of the sphere (tiles or spherical polygons) that remain

after removing the points and arcs corresponding to the embedding. Faces are not necessarily topological disks (there can be holes). For example, a disconnected graph has at least one non-disk face.

*Stress.* Let  $N(i)$  denote the set of edges incident to a vertex  $i \in V$ . Let  $u_{i,e}$  be the unit vector tangent to the geodesic arc corresponding to the edge  $e \in E$  at the point  $p_i$ , oriented towards the edge, as illustrated in Fig. 29. An *equilibrium stress* on a spherical embedded graph is a map

$$s: E \rightarrow \mathbb{R}$$

from the edges to the reals which satisfies the *equilibrium condition* at every vertex  $i \in V$ :

$$\sum_{e \in N(i)} s_e u_{i,e} = 0. \quad (4)$$

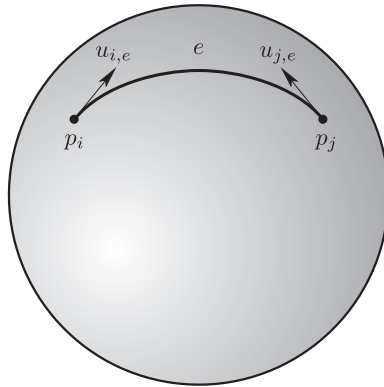


Figure 29. Vectors  $u_{i,e}$  used in defining spherical stress.

By definition, we also assign a stress, which can be any number, to the edge of the single-loop graph.

A stress is *non-trivial* if it is not identically zero. A stress is *non-zero* if it is non-zero on every edge.

*Remark.* This definition is a slight modification of the similar concept used by Maxwell [26] for planar graphs and adjusted here for the sphere. The intuition behind it comes from imagining the edges as springs lying on the sphere (or, as in Maxwell's paper, in the plane). Depending on whether they are stretched or compressed compared to their natural state, the system of springs associated to a graph is in equilibrium exactly when condition (4) holds. The vector  $s_e u_{i,e}$  equals the force applied at the point  $p_i$  by the spring along the edge  $e$ .

In drawing such graphs, we colour in red the positively stressed edges, that is, those with  $s(e) > 0$ . Negatively stressed edges are coloured in blue.

The following proposition gives the important correspondence between convex polytopes and spherical (positively) stressed graphs (see Fig. 30).

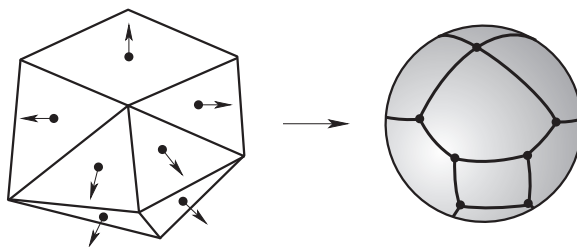


Figure 30. A convex polytope yields a graph with positive equilibrium stress.

**Proposition 18.** *Let  $K \subset \mathbb{R}^3$  be a convex polytope. Its spherical fan yields a spherical embedded graph  $G_K$  whose edges correspond (by duality) to edges of the polytope  $K$ . Let the function  $s_K$  send each edge of  $G_K$  to the length of the corresponding edge of  $K$ . Then  $s_K$  is a positive equilibrium stress of  $G_K$ . Conversely, each spherical positively stressed graph uniquely defines a convex polytope  $K \subset \mathbb{R}^3$ .*

This representation includes a single-vertex polytope (represented by the empty graph), the two-vertex polytope (the line segment) represented by a single-loop graph, and all ‘flat’ polytopes (that is, convex polygons) represented by graphs with two antipodal vertices and at least three edges.

Now we turn the set of non-zero stressed graphs into a group.

*Sum of stressed graphs.* The sum  $(G, s) = (G_1, s_1) + (G_2, s_2)$  of two spherical equilibrium stressed graphs is defined via the following algorithm.

**Algorithm** (sum of two spherical stressed graphs; see Figs. 31 and 32).

1. Each of the graphs yields a tiling of the sphere  $S^2$ . We take a graph  $G$  yielding their common refinement: it may have new vertices, and some of the original edges may get split.
2.  $G$  has a natural stress defined as the sum of  $s_1$  and  $s_2$ , as follows. Let  $e \in E$  be an edge of  $G$ . If it lies on some edge of  $G_1$  but on no edge of  $G_2$ , then we assign to  $e$  the stress  $s_1$  (similarly, an edge lying on some edge of  $G_2$  but on no edge of  $G_1$  inherits the stress  $s_2$ ). If  $e \in E$  lies on an edge of  $G_1$  and on an edge of  $G_2$ , then we take the sum of the inherited stresses. The stress obtained is not necessarily non-zero, so we need some further reductions.
3. Remove all zero-stressed edges of  $G$ . Remove isolated vertices.
4. If vertices of degree two exist, then the two adjacent edges must form an angle of  $\pi$  and be equally stressed. In this case, we remove the vertex and collapse its two incident edges into one.

*Properties of addition of stressed graphs.* The following properties are immediate consequences of the above algorithm: (a) the zero element with respect to addition is the empty graph; (b) the addition of positively stressed graphs corresponds to Minkowski addition of the associated convex polytopes; (c) each stressed graph has an *inverse*, obtained by simultaneously negating the signs of all its edges; (d) the group of non-zero stressed graphs is generated by the positively stressed graphs.



Figure 31. The sum of two positively stressed graphs.

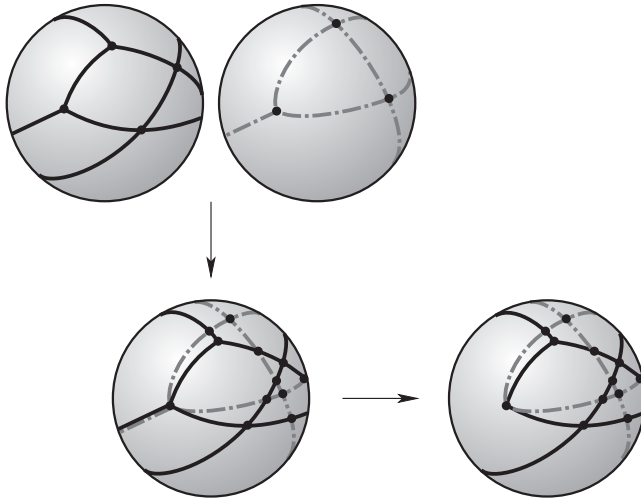


Figure 32. The sum of two stressed graphs with one positively stressed and the other negatively stressed.

From this, we immediately obtain the following.

**Theorem 19** ([23]). *The group of non-zero stressed graphs is canonically isomorphic to the group of virtual polytopes. The canonical isomorphism sends a formal difference  $K_1 \otimes K_2^{\otimes -1}$  of convex polytopes to the difference*

$$(G_1, s_1) - (G_2, s_2)$$

*of the associated (positively) stressed graphs.*

This allows us to speak of *virtual polytopes represented by stressed graphs*.

*Historical notes.* The material in this section comes from Panina [23]. An advantage of the representation is that it helps to construct virtual polytopes in dimension three by just drawing pictures on the sphere.

**5.2. Virtual polytopes represented by Maxwell polytopes.** In this subsection we turn to a new representation of 3D virtual polytopes as *Maxwell polytopes*. This is the closest in spirit to the theory of polytopes. We already have some intuition concerning non-convexity and self-intersections coming from coloured polygons in dimension two.

We show how a virtual polytope can be represented as a Maxwell polytope together with an associated fan, and we discuss properties of this representation. Finally, in particular, we discuss the problem of detecting which Maxwell polytopes represent virtual polytopes and which do not, a problem that extends to dimension three the similar discussion in §3.3 (which polygons represent virtual polytopes and which do not).

*Face graphs and their duals.* By a *graph*  $G = (V, E)$  we mean the same object as in the previous section. Recall that we allow loops and multiple edges, also a single-loop graph, that is, one loop edge with no vertices on it.

A *cycle*  $(v_1, e_1, v_2, e_2, \dots, e_n, v_{n+1})$  of length  $n \geq 2$  in a graph is a circular sequence<sup>6</sup> of vertices and edges, with  $v_1 = v_{n+1}$  and  $e_i = \{v_{i-1}v_i\}$ . Loops with a single vertex or without vertices are also cycles, of length one and zero, respectively. A cycle is *edge simple* if there are no edge repetitions.

A *face* is a non-empty set of edge-simple cycles in  $G$  without common edges.

**Definition 10.** A *face graph* is a graph  $G$  together with a (finite) collection of faces  $C_1, \dots, C_m$ , where we assume that no edge appears in the cycles of  $C_i$  more than twice.

We visualize a face graph as a (combinatorial) surface (possibly with holes). Indeed, we can patch up each of the sets  $C_i$  of cycles. If a set  $C_i$  consists of a unique cycle, we imagine a disk patching up the cycle. If the face consists of  $k \geq 2$  cycles, then we imagine a (topological) sphere with  $k$  holes patched to them (each cycle bounding a hole). A *spherical face graph* is a face graph whose associated surface is the sphere.

**Definition 11.** The dual  $G^* = (V^*, E^*, F^*)$  of a non-crossing spherical face graph  $G = (V, E, F)$  has  $V^* = F$ ,  $F^* = V$ , and  $E^* = E$ . Two dual vertices (corresponding to two primal faces) are connected by a dual edge whenever the primal faces share an edge.

The dual of a spherical face graph is not necessarily a spherical graph, but it is always a *cactus of spheres*, defined below.

*A cactus of spheres.* This surface (with singularities) is defined inductively. The base case is a combinatorial sphere. At each inductive step, we attach a new sphere at an existing vertex. Underlying the cactus is a tree-like structure, as illustrated in Fig. 33. The tree has a node for each sphere, and a tree edge joins two nodes whose corresponding spheres share a point.

We will only be interested in face graphs dual to spherical stressed graphs.

*Embedded graph and its faces.* For an embedded spherical graph  $G$ , the embedding defines the faces as the connected components of the complement of the edges and vertices. The boundary of a face is a collection of cycles in the graph  $G$ . If  $G$  is a connected graph, then all the faces are disks. Otherwise there may be faces that are topologically spheres with holes. We assume that the cycles are consistently

---

<sup>6</sup>A finite ordered list of elements considered up to a power  $(2, 3, \dots, n, 1)^k$  of the cyclic permutation.

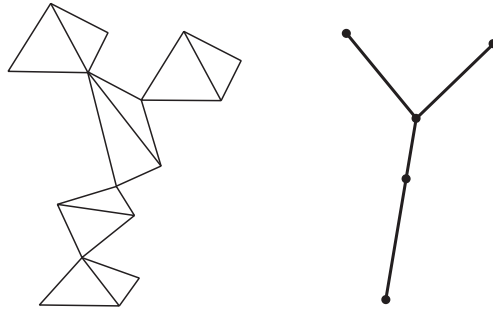


Figure 33. A cactus graph and its underlying tree.

oriented, for example, so that a disk-like face lies ‘on the left-hand side’ of its boundary cycle.

The faces of a stressed graph are the connected components of elements of the spherical fan (see Definition 8) of the corresponding virtual polytope.

**Definition 12.** Given a virtual polytope  $K$  represented by a stressed graph  $(G, s)$ , its *reduced spherical fan* is the face graph generated by  $G_K$  (see Fig. 34).

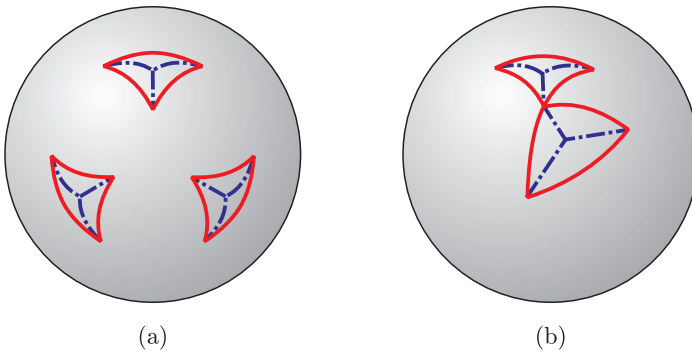


Figure 34. (a) Faces of the fan are not necessarily disks. (b) A self-touching face.

*Dual of a spherical face graph.* The following properties result from direct application of the above definition to the kind of spherical graphs that support a non-zero stress.

- 1) All the faces of the dual face graph are topological disks.
- 2) If the graph is connected, then its dual is a topological sphere.
- 3) If the graph has  $k$  connected components, then the dual graph has the topology of a cactus of  $k$  spheres.

*Maxwell polytopes.* With these concepts in place, we turn to one of the main definitions of this subsection.

**Definition 13.** A *Maxwell polytope* is a face graph together with a (not necessarily injective) map of the vertices to  $\mathbb{R}^3$  such that the following hold.

- 1) *Non-degeneracy of edges:* the endpoints of each edge are mapped to distinct points.
- 2) *Face planarity:* the vertices of each face are mapped to coplanar points. Thus, each face is mapped to a planar (possibly self-intersecting) polygon.
- 3) *Non-degeneracy of faces:* the vertices of each face are not mapped to collinear points. In other words, the image of a face defines a unique plane.

The images of the vertices, edges, and faces of the face graph are called *vertices*, *edges*, and *faces of the Maxwell polytope*.

By the *combinatorics of a Maxwell polytope* we mean the underlying face graph.

*Virtual polytopes as Maxwell polytopes.* Let us consider a virtual polytope  $K$  which is neither a segment nor a point. We have seen in §2.3 that a virtual polytope has faces which are themselves virtual polytopes of a lower dimension. Thus, a three-dimensional virtual polytope  $K$  has vertices, edges, and (two-dimensional) facets.

We make use of the representation of  $K$  as the support function  $h$ , which comes together with the reduced spherical fan  $\Sigma$ . We also use the representation of  $K$  as a spherical stressed graph  $(G, s)$ .

**Definition 14.** The *Maxwell polytope  $M$  associated to the virtual polytope  $K$*  is defined as follows.

- 1) The underlying face graph is dual to the reduced spherical fan  $\Sigma$ , or, equivalently, dual to the face graph induced by the stressed graph  $G$ .
- 2) The vertices of  $M$  are vertices of  $K$ : each vertex of the dual face graph  $\Sigma^*$  corresponds to a face of  $\Sigma$ , which is a linearity domain of the support function and therefore corresponds to a vertex of  $K$ .

We now analyze in detail the vertices, edges, and faces of the Maxwell polytope associated to a virtual polytope.

*Vertices.* By definition, the vertices of  $M$  are the vertices of  $K$ .

*Edges.* By Theorem 1, a vertex of an edge of  $K$  is a vertex of  $K$ . Therefore, edges of  $K$  connect vertices. Since they are one-dimensional virtual polytopes, that is, virtual segments, we represent them by blue and red segments, as discussed in §2. An edge of  $K$  corresponding to an edge  $e$  of the graph  $G$  is a segment which is orthogonal to the affine hull of  $e$  and has length equal to the absolute value of the stress. The colour of the edge is determined by the sign of the stress.

*Facets.* Some of the edges form closed planar coloured polygons that represent facets of  $K$ . These are also faces of  $M$ .

*Remark.* A virtual polytope  $K$  and the centrally symmetric image  $\text{Symm}(K^{\otimes -1})$  of its inverse yield one and the same Maxwell polytope, but with reversed colourings.

**Algorithm 20** (stressed graph to Maxwell polytope (for connected graphs)). Let  $K$  be a virtual polytope represented by a stressed connected graph  $(G, s)$ . The associated Maxwell polytope is retrieved as follows.

1. Let  $p_i$  be a vertex of  $G$ , viewed as a unit vector emanating from the center of the sphere, and take the plane  $\pi$  orthogonal to  $p_i$ . Since it is oriented by the direction of  $p_i$ , we can speak of clockwise and counterclockwise rotations in this plane.

2. The star (in  $G$ ) of the vertex  $p_i$  induces a coloured star in  $\pi$ .

3. In turn, this coloured star defines a coloured polygon  $P$  in  $\pi$  (as in §3.1).

4. After a clockwise rotation of  $P$  through an angle  $\pi/2$ , we obtain the face  $K^{p_i}$  represented by a coloured polygon.

5. The above steps retrieve all the faces up to a translation. The combinatorics of the graph  $(G, s)$  indicates which faces should share an edge. We shift the faces by parallel translations so as to have the required incidence relations as follows: start with one face and fix its position. The positions of the adjoining faces are uniquely determined. Since the graph  $G$  is connected, the positions of all the facets are determined.

Before considering arbitrary stressed graphs (with several connected components), we look at one particular example.

**Example 12.** A stressed graph with two connected components and its corresponding Maxwell polytope are illustrated in Fig. 35. The Maxwell polytope is represented as a gluing together vertex-to-vertex of the two Maxwell polytopes corresponding to the connected components.

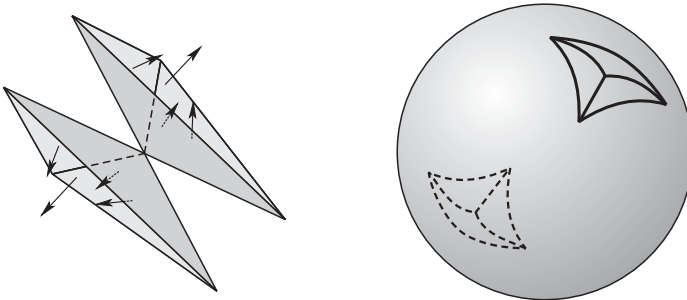


Figure 35. The Maxwell polytope on the left is associated to the disconnected spherical stressed graph on the right.

A disconnected stressed graph  $(G, s)$  splits into the disjoint union of its connected components  $G_i$ . Each component can be treated as a separate virtual polytope represented by a stressed graph, and therefore gives a Maxwell polytope  $M_i$  which is a topological sphere. These polytopes are then glued together vertex-to-vertex to form a Maxwell polytope of the graph  $(G, s)$ .

In more detail, we have the following algorithm.

**Algorithm 21** (stressed graph to Maxwell polytope (for disconnected graphs)). Let  $K$  be a virtual polytope represented by a stressed graph  $(G, s)$ .

1. Decompose  $G$  into the union of its connected components  $G_i$ . Each connected component comes together with a spherical embedding inherited from  $G$

and with the stress inherited from  $(G, s)$ . For each of the connected components, apply Algorithm 20 and construct the corresponding Maxwell polytope  $M_i$  (up to a translation).

2. Whenever  $G_i$  and  $G_j$  have edges incident to the same face  $F$ , the corresponding Maxwell polytopes  $M_i$  and  $M_j$  should share the vertex that corresponds by duality to  $F$ . This determines the relative position of  $M_i$  and  $M_j$  and, eventually, recovers the cactus structure for  $M$ .

**5.3. Detecting virtual polytopes.** In this section we consider the problem of detecting which Maxwell polytopes correspond to virtual polytopes. We restrict the discussion to connected face graphs, whose duals are topological spheres (rather than cactuses). The general case of disconnected graphs follows immediately. We start by analyzing the case of trivalent stressed graphs.

*Simplicial virtual polytopes in 3D.* Let us consider a 3D virtual polytope  $K$  represented by a stressed connected trivalent graph  $(G, s)$ : each vertex of  $G$  is incident to exactly three edges. Then each face of the associated Maxwell polytope is a virtual triangle, that is, a triangle with some colouring on the edges. Two triangles are patched together edge to edge whenever the corresponding vertices of the graph are connected by an edge. In other words, the Maxwell polytope  $M$  that represents  $K$  is a *simplicial surface in  $\mathbb{R}^3$* . Hence, we refer to this kind of virtual polytope  $K$  as a *simplicial virtual polytope*. A number of simplicial virtual polytopes with particular geometrical and combinatorial properties are illustrated in Example 16, Fig. 37, and Fig. 43.

*Detecting simplicial virtual polytopes.* Let  $M$  be any sphere-homeomorphic simplicial surface in  $\mathbb{R}^3$ . We do not require  $M$  to be embedded or even immersed, and thus the surface may have both global and local self-intersections, but we do require that no two adjacent triangles lie in the same plane.

As a counterpart of Definition 3 we define the following concept.

**Definition 15.** A Maxwell polytope is a *v-polytope* if it is associated to some virtual polytope.

Most simplicial surfaces are not v-polytopes. The answer to the natural question of *when a given simplicial surface  $M$  is a v-polytope* is given algorithmically.

**Algorithm 22** ([24] Is a simplicial surface a v-polytope?).

Let  $M$  be a simplicial surface.

1. Choose a normal vector to each of the (triangular) facets. This can be done independently, that is, we do not require that the collection of all normal vectors yields a global orientation of  $M$ . The normal vectors for different facets should be different. If this is not possible, then there is no virtual polytope associated to the surface.

2. Mark the endpoints of all the normal vectors on the unit sphere  $S^2$ .

3. Whenever two marked points correspond to two adjacent facets of  $M$ , connect them by a geodesic arc (an edge). We may choose either the short or the long arc. The result should be an embedded graph, that is, these edges must not intersect. If we succeed, then we have obtained a spherical fan  $\Sigma$ .

4. If no such assignment of normal vectors or no embedded graph can be found, then we conclude that there is no virtual polytope associated to the surface.

5. Otherwise, each such fan  $\Sigma$  together with the surface  $M$  gives a virtual polytope  $K$  represented by the pair  $(M, \Sigma)$ .

We emphasize that different fans on the same surface induce different virtual polytopes. The spherical fan  $\Sigma$  is the reduced spherical fan of the virtual polytope  $K$  found to be compatible with the given surface  $M$ . For a vertex  $p$  of  $M$  and a face  $A$  of  $\Sigma$  related to  $p$  by duality, the restriction of the support function  $h_K$  to the cone  $A$  is the (globally) linear function represented by the scalar product  $\langle p, x \rangle$ .

The colouring of the edges of  $M$  is superfluous in  $(M, \Sigma)$ : it is uniquely recovered from the pair  $(M, \Sigma)$ .

*Ambiguous v-polytopes.* A Maxwell polytope is called an *ambiguous v-polytope* if it supports at least two non-complementary virtual polytope colourings. An example is provided by the surface of a tetrahedron, which is very ambiguous: there exist 52 virtual polytopes associated to it (see Example 13 in §5.4).

*The general case: non-trivalent stressed graphs.* We turn now to the general case. If a virtual polytope  $P$  is represented by a non-trivalent stressed graph, then its Maxwell polytope is not a simplicial surface. In fact, it may not be a piecewise linear surface at all, since the polygons representing the faces may have self-intersections.

An extension of the previous algorithm can determine when a Maxwell polytope is a v-polytope. The algorithm is almost the same, except for an additional case needed to treat antipodal points that should be connected by an edge.

**Algorithm 23** (is a Maxwell polytope a v-polytope?). Let  $M$  be an uncoloured Maxwell polytope.

1. Choose a normal vector to the affine hull of each of the facets of  $M$ . (We do not require the set of normal vectors to define a global orientation of  $M$ .) The normal vectors for different facets should be different. If this is not possible, then there is no associated virtual polytope.

2. Proceed as in Algorithm 22. A necessary addendum is the following: assume that two antipodal points correspond to two adjacent faces sharing an edge  $e$ . These two points also should be connected by an edge, but this time with the extra condition that the connecting arc on the sphere should be orthogonal to the affine hull of  $e$ . Again, we can choose between two options: we can take either one or the other semicircle.

3. If we end up with a fan  $\Sigma$ , then  $\Sigma$  and the surface  $M$  together give a virtual polytope  $K$  represented by  $(M, \Sigma)$ .

The orthogonality condition here is necessary. It has been discussed in §5.2.

Thus, we can speak of virtual polytopes represented by a Maxwell polytope  $M$ , together with an associated reduced fan  $\Sigma$ .

**5.4. Examples of virtual polytopes in dimension three.** We now present a collection of virtual polytopes in dimension three. According to Algorithm 23 each of the examples presents a virtual polytope as a Maxwell polytope together with an associated fan.

**Example 13** (the tetrahedron is v-ambiguous). There exist 52 different virtual polytopes associated to the surface of a convex tetrahedron. We depict three of them separately in Fig. 36, and give the complete list in Fig. 37. The second tetrahedron in Fig. 36 represents the family of hyperbolic virtual polytopes, to be defined and discussed in § 6.1.

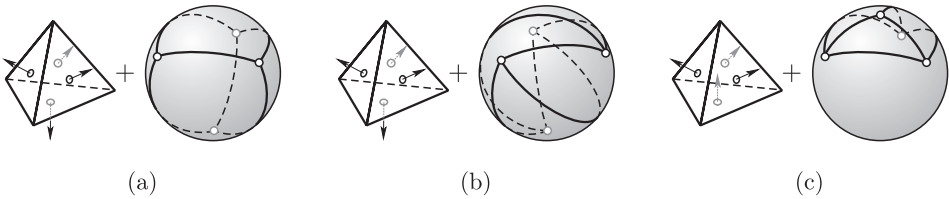


Figure 36. (a) Convex tetrahedron. (b) Hyperbolic tetrahedron. (c) Yet another virtual tetrahedron.

**Example 14** (a v-polytope with self-intersecting faces). Figure 38 shows a virtual polytope with self-intersecting faces.

**Example 15** (a v-polytope with a two-connected vertex-edge graph). The vertex-edge graph of a virtual polytope is always connected. Balinski's theorem [27] states that the vertex-edge graph of a convex three-dimensional polytope is three-connected, that is, the removal of any 2 vertices together with the edges adjacent to them leaves the graph connected. We have already seen in Fig. 35 that the vertex-edge graph of a virtual polytope can fail to be two-connected. Figure 39 presents a virtual polytope whose vertex-edge graph is two-connected but not three-connected.

**Example 16** (a flexible v-polytope). Cauchy's theorem states that three-dimensional convex polytopes are never flexible. However, if the convexity condition is omitted, then there exist flexible simplicial surfaces. We need here Bricard's flexible octahedron of the second type, which is a self-intersecting polygon, a combinatorial octahedron. It can be constructed as follows: inscribe in a circle a self-intersecting closed polygon with edge lengths  $a, b, a, b$ . The vertices of the polygon will serve as four vertices of Bricard's octahedron, and the edges of the polygon will be edges of the octahedron. As the remaining two vertices we take two points equidistant from the plane of the circle and lying on opposite sides of the plane and such that their projections on the plane coincide with the center of the circle. Joining the six vertices by edges according to octahedral combinatorics, we get Bricard's flexible octahedron of the second type. The Bricard octahedron in Fig. 40 has an associated fan constructed according to Algorithm 22.

More sophisticated examples of virtual polytopes will be given in § 6.1.

**5.5. Support functions and liftings of stressed graphs.** The support function representation of a virtual polytope is very closely related to the stressed

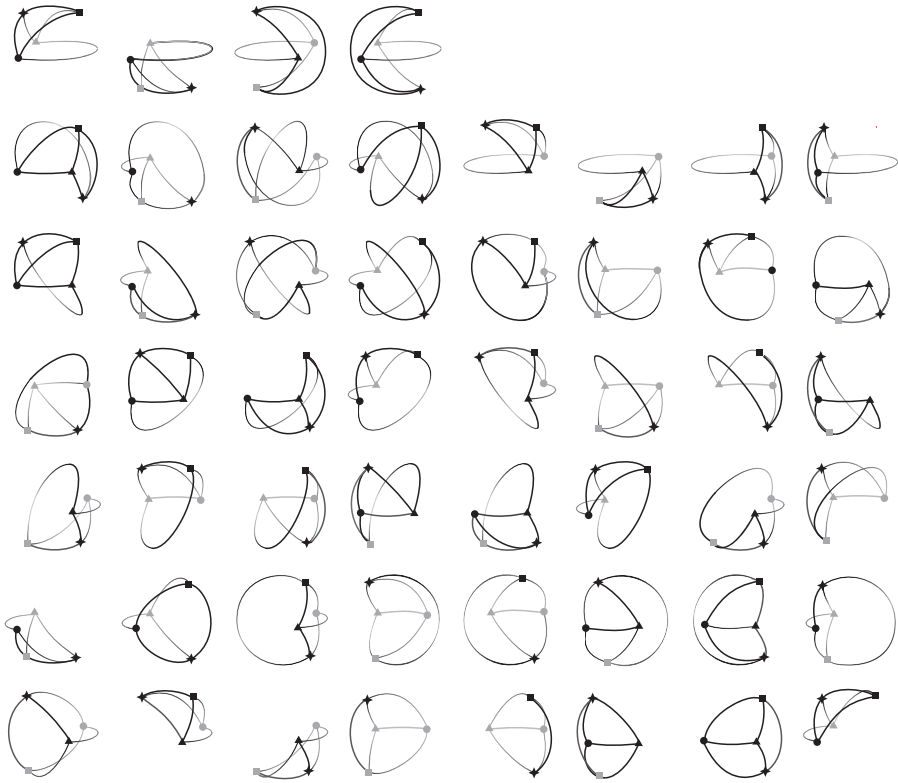


Figure 37. All 52 virtual tetrahedra. We depict here only their fans. (Picture by Vlad Sherbina.)

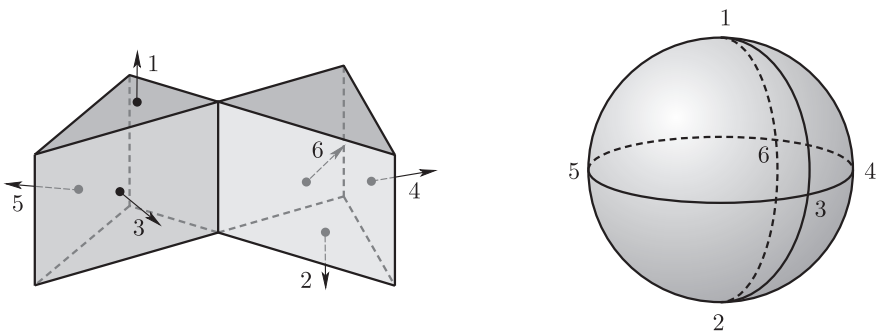


Figure 38. Self-intersecting virtual polytope.

graph representation. For completeness, we give two algorithms converting one to the other and following from Lemma 12.

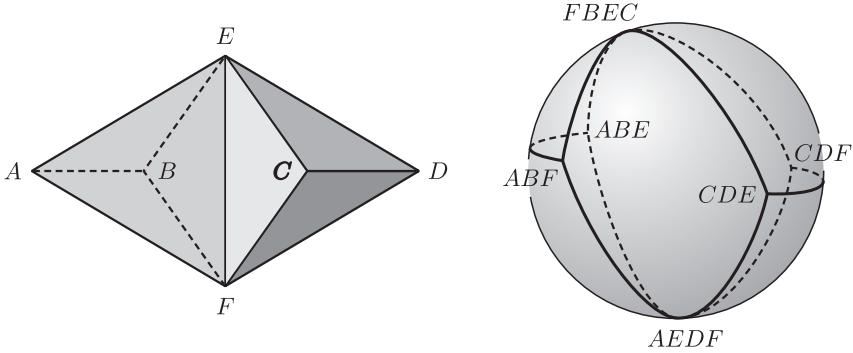


Figure 39. Virtual polytope whose vertex-edge graph is not 3-connected.

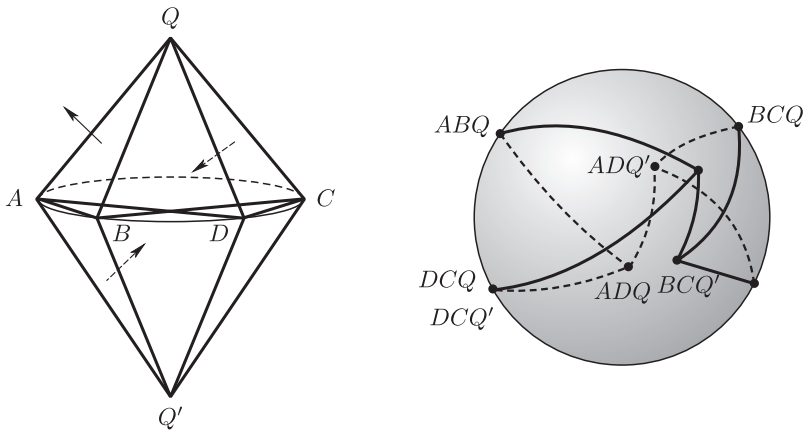


Figure 40. Bricard's octahedron is a flexible virtual polytope. The octahedron is shown together with the normal vectors of the faces (left) and its fan (right).

**Algorithm 24** (support function to stressed graph). Let the virtual polytope  $K$  be represented by its support function  $h$ . Then the corresponding stressed graph  $(G, s)$  is retrieved as follows:

1. The linearity domains of  $h$  form the fan associated to  $K$ . Intersecting the fan with the unit sphere, we get an embedded graph  $G$ . It remains to recover the stress.
2. Take an edge  $e$  of the graph  $G$ . It is adjacent to two faces that correspond to two cones  $\sigma_1$  and  $\sigma_2$  in the fan. The two cones share a face  $F = \sigma_1 \cap \sigma_2$ . By construction, the function  $h$  is linear on each of the cones. Let  $h = \langle p_1, \cdot \rangle$  on  $\sigma_1$  and  $h = \langle p_2, \cdot \rangle$  on  $\sigma_2$ .
3. Let the stress on the edge  $e$  equal the scalar product  $\langle p_1 - p_2, v \rangle$ , where  $v$  is the unit outward normal vector to the face  $F$  of the cone  $\sigma_1$  (see Fig. 41).

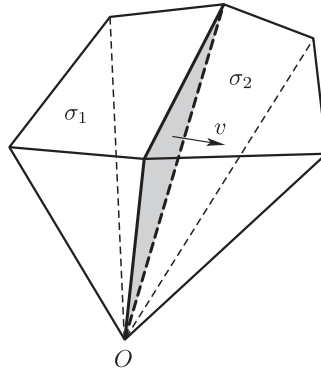


Figure 41. The normal vector to the common face of two adjacent cones in a fan.

**Algorithm 25** (stressed graph to support function). Conversely, given a stressed graph  $(G, s)$ , the corresponding support function of a virtual polytope is retrieved as follows.

1. The embedded graph  $G$  yields a fan  $\Sigma$ .
2. We construct a function  $h$  which is piecewise linear with respect to  $\Sigma$ : choose one of the three-dimensional cones of the fan, say  $\sigma_1$ , and set  $h$  equal to zero on  $\sigma_1$ .
3. Take a cone  $\sigma_2$  which shares a face  $F$  with  $\sigma_1$ . The face corresponds to an edge  $e$  of the graph  $G$ . Define the restriction of  $h$  to the cone  $\sigma_2$  as

$$h|_{\sigma_2} = h|_{\sigma_1} + s(e)\langle v, \cdot \rangle.$$

Here again  $v$  is the unit outward normal vector to the face  $\sigma_1 \cap \sigma_2$  of the cone  $\sigma_1$  (see Fig. 41), and  $s(e)$  is the value of the stress on the edge  $e$ .

4. Continue taking adjacent cones one by one, in an arbitrary order.

*Maxwell's correspondence.* We now relate the previous discussion about *support functions versus stressed graphs* to the (old and classical) construction in rigidity theory about *lifting versus stress*, as introduced by Maxwell in [26].

Assume that we have a graph  $G$  embedded in the plane  $\mathbb{R}^2$  so that the edges are realized by line segments. This gives a tiling of the plane into regions (some of them are bounded, one is not). A *lifting* of the embedded graph is a continuous function  $h: \mathbb{R}^2 \rightarrow \mathbb{R}$  which is piecewise linear with respect to the tiling. The graph (in other terminology, the *terrain*) of  $h$  is a piecewise linear surface.

Each embedded graph has a *trivial lifting* which is a (globally) linear function. However, not all graphs have non-trivial liftings. It was James Clerk Maxwell who observed in [26] that liftability is directly related to the existence of an equilibrium stress on the embedded graph. He presented a way of reconstructing a lifting from a stress and vice versa. This is referred to as *Maxwell's correspondence*. More precisely, Maxwell established an isomorphism between the linear space of all liftings factorized by globally linear functions and the space of equilibrium stresses of the same graph.

In the above algorithms we adopted the approach used by Maxwell.

There exists yet another relationship between support functions and liftings of planar graphs. Assume that we have a virtual polytope, which, as we know, comes with its support function  $h$ , also represented by a spherical stressed graph  $(G, s)$ . Take a plane  $e \subset \mathbb{R}^3$  and intersect it with the fan. The intersection  $\bar{G}$  equals the central projection on  $e$  of a hemispherical part of  $G$ . It resembles an embedded graph except with the difference that some edges may go to infinity. We can extend Maxwell's lifting to this kind of object by literally repeating the definition. Then the restriction of the support function  $h_K$  to the plane  $e$  is a lifting of  $\bar{G}$ .

## 6. Applications

In this section we demonstrate the usefulness of the theory of virtual polytopes with a selection of problems and applications originating in various areas of mathematics.

**6.1. A. D. Alexandrov's problem and hyperbolic virtual polytopes.** A necessary warning: hyperbolic polytopes are not polytopes lying in some hyperbolic space, but rather a special subclass of 3D virtual polytopes.

We introduce *hyperbolic virtual polytopes*, or, shortly, *hyperbolic polytopes*. This class of virtual polytopes emerged naturally from a number of geometry problems in the style of Alexandrov, and it has been used to provide new insights into one of his theorems concerning 3D polytopes, and to resolve one of his longstanding conjectures.

The underlying idea for the results presented in this section is that hyperbolic polytopes, while retaining many of the properties of convex ones, lie almost at the opposite pole in terms of convexity properties. A generic virtual polytope is somewhere convex, somewhere concave, and somewhere saddle-like: hyperbolic ones are totally saddle-like.

To make this precise, we rely on the following definition (illustrated in Fig. 42) of saddle surfaces, which makes sense in both the smooth and the piecewise linear case.

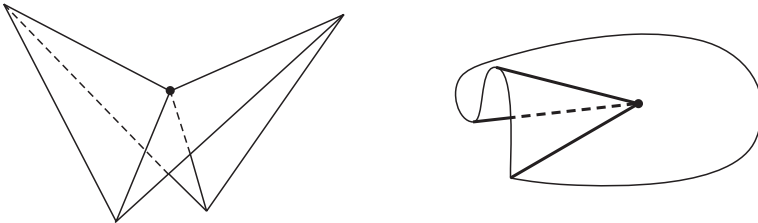


Figure 42. Saddle points on surfaces.

**Definition 16.** Let  $F$  be a surface in  $\mathbb{R}^3$ . A point  $x \in F$  is called a *saddle point* if no plane passing through  $x$  intersects  $F$  locally at just one point. The surface is a *saddle surface* if all its points are saddle points.

To define hyperbolic virtual polytopes, we need the following preliminary construction. Let  $K$  be a virtual polytope in  $\mathbb{R}^3$ , and let  $h$  be its support function. For a vector  $v \in S^2$ , the equation

$$\langle x, v \rangle = 1$$

defines a plane  $e(v)$ . We consider the restriction of  $h$  to  $e(v)$  and denote by  $\mathcal{F}_v$  the graph of this restriction. The surface  $\mathcal{F}_v$  is piecewise linear. Its vertices and edges correspond to those of the fan  $\Sigma_K$  that lie in the open hemisphere with pole at  $v$ .

Since convex polytopes are those virtual polytopes that have convex support function, we conclude that a virtual polytope is convex (that is,  $K \in \mathcal{P}$ ) if and only if the surface  $\mathcal{F}_v$  is convex for any  $v$ . In analogy to this property, we give the following definition.

**Definition 17.** A virtual polytope  $K$  is said to be *hyperbolic* if  $\mathcal{F}_v$  is a saddle surface for any  $v \in S^2$ .

The theory of hyperbolic polytopes emerged originally as a tool for constructing counterexamples to the following uniqueness conjecture, proved by Alexandrov [2] in the case of analytic surfaces.

**A. D. Alexandrov's problem** (uniqueness of smooth convex surfaces). *Let  $K \subset \mathbb{R}^3$  be a smooth convex body, and let  $R_1(x)$  and  $R_2(x)$  be the principal curvature radii of its boundary  $\partial K$  at the point  $x$ . If there is a constant  $C$  such that*

$$R_1(x) \leq C \leq R_2(x)$$

*at every point of  $\partial K$ , then  $K$  is a ball.*

For general (not necessarily analytic) smooth surfaces, the problem remained open for a long time, until Martinez-Maure gave a first  $C^2$ -counterexample in 2001 [28].

Subsequently, Panina presented a series of  $C^\infty$ -counterexamples and developed a systematic theory, based on hyperbolic virtual polytopes, for constructing an infinite class of such counterexamples. Details can be found in [24], [29], and further illustrations and three-dimensional electronic models in [30].

*Panina's construction.* To produce counterexamples to Alexandrov's problem, we need a simplicial hyperbolic virtual polytope with the additional property that the edges of its spherical fan are all shorter than  $\pi$ . Since hyperbolic polytopes are rare phenomena among virtual polytopes, the construction of such an object is a challenging step. Next, we show that the support function  $h$  of the constructed hyperbolic virtual polytope can be smoothed. More precisely, there exists a  $C^\infty$ -smooth saddle function  $h'$  which approximates  $h$ . The smoothing technique works only for virtual polytopes with the above additional property.

Now let  $h_R$  be the support function of the ball of radius  $R$ . If the sum  $h' + h_R$  is a convex function (for this purpose  $R$  should be sufficiently large), then  $h' + h_R$  is the support function of some smooth convex body  $K'$  which is a counterexample.

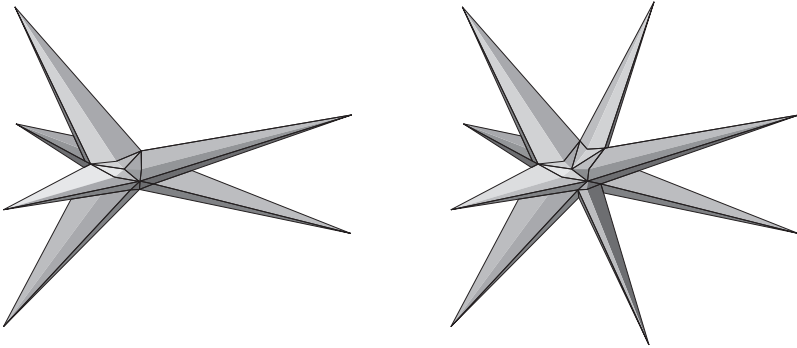


Figure 43. Two hyperbolic virtual polytopes represented by Maxwell polytopes: (left) with six horns and (right) with eight horns.

*Constructing hyperbolic polytopes.* We first describe a convenient criterion for hyperbolicity of virtual polytopes.

**Definition 18.** A vertex  $p$  of a spherical fan  $\Sigma$  is *pointed* if there exists an angle larger than  $\pi$  incident to  $p$ . A fan is *pointed* if all of its vertices are pointed.

**Lemma 26.** *If  $K$  is a virtual polytope with a pointed spherical fan  $\Sigma_K$ , then  $K$  is hyperbolic.*

**Example 17.** The *hyperbolic tetrahedron* in Fig. 36 (b) is a hyperbolic virtual polytope.

Advanced examples of hyperbolic virtual polytopes appeared in [24] and [29]. They are represented by explicitly described Maxwell polytopes and are hyperbolic by Lemma 26 because their fans are pointed by construction. This is illustrated in Figs. 43 and 44.

*A. D. Alexandrov's uniqueness theorem for convex polytopes and its refinements.* Here is one more application of hyperbolic virtual polytopes (see [31]). It is related

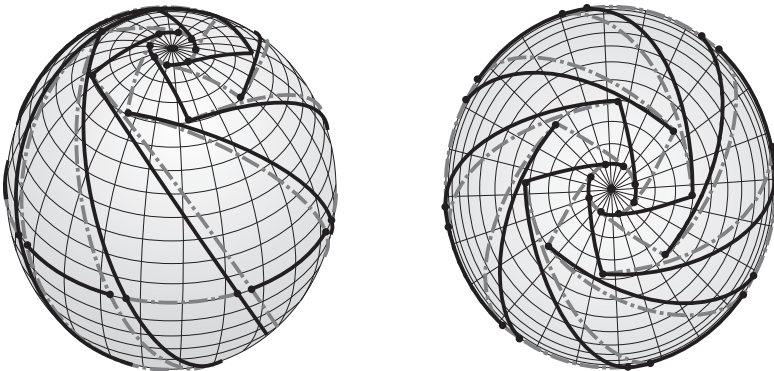


Figure 44. Fan of the hyperbolic polytope with eight horns.

to the following theorem regarded by Alexandrov as a discrete counterpart of the aforementioned theorem on the uniqueness of smooth convex surfaces [2].

**Theorem 27** (uniqueness theorem for convex polytopes [2]). *Let  $K$  and  $M$  be three-dimensional convex polytopes. If for any pair of their parallel facets, neither can be moved strictly inside the other via a translation, then the polytopes coincide up to a translation.*

Since this theorem is related to Alexandrov's problem, it is not surprising that it has a natural interpretation in terms of hyperbolic polytopes. Moreover, a little deeper understanding of hyperbolic polytopes leads to the following two refinements of the theorem.

**Theorem 28** ([31]). *There exist two different three-dimensional convex polytopes  $K$  and  $L$  such that for any pair of their parallel facets, there is **at most one** translation which moves one of them strictly inside the other.*

The example is far from trivial. For its construction, we need a hyperbolic polytope with the additional property that its fan admits a regular triangulation without adding extra vertices (Steiner points).

**Theorem 29** ([31]). *Let  $K$  and  $L$  be three-dimensional convex polytopes. Suppose that for each pair of parallel facets:*

- 1) *there exists **at most one** translation  $t$  moving the facet of  $K$  into the facet of  $L$ ;*
- 2) *there exists **no** translation  $t$  moving the facet of  $L$  into the facet of  $K$ .*

*Then the polytopes coincide up to a translation.*

There is one more recent result in this direction (see [32]). It describes two convex polytopes in  $\mathbb{R}^3$  such that for each pair of their parallel facets, the facets are different, and there exists **exactly one** translation moving one of them into the other.

*Hyperbolic virtual polytopes and pointed tilings.* Between the theory of hyperbolic virtual polytopes and the theory of *pointed tilings* [33] there is a relationship which highlights the above constructions. In a sense, planar pointed tilings (defined below) are opposite to the more traditional convex graph embeddings: they are as non-convex as possible. As a parallel phenomenon, hyperbolic virtual polytopes also are as non-convex as possible. The two theories have an overlap to be sketched now. For details, we refer the reader to [23].

A *pseudotriangle* is a closed polygon without self-intersections with exactly three angles smaller than  $\pi$ . All other angles are reversed. Originally, a pseudotriangle is defined to be a planar polygon, but the definition extends to spherical polygons as well. A *pseudotriangulation* is a partition of a region of the plane (or of the sphere) into pseudotriangles. A *pointed tiling* is a tiling such that each vertex has an adjacent angle greater than  $\pi$ . Alternatively, a pointed pseudotriangulation on the plane can be defined as a finite non-crossing collection of line segments such that at each vertex there is an adjacent angle greater than  $\pi$ , and such that no line segments can be added between any two existing vertices while preserving this property.

Pointed pseudotriangulations on the plane were first considered by Streinu [34], [35] as part of her solution to the carpenter’s ruler problem, a proof that any simple polygonal path in the plane can be straightened out by a sequence of continuous motions. A crucial property used by Streinu in the proof is that a pointed tiling has only the trivial stress.

Pointed pseudotriangulations satisfy the conditions defining a *Laman graph*: such a graph has exactly  $2v - 3$  edges, (where  $2v$  is the number of vertices) and every  $k$ -vertex subgraph has at most  $2k - 3$  edges. This follows directly from the Euler formula. Simple dimension counts show that for a generically embedded graph, a necessary and sufficient condition for there to exist a non-trivial stress is that the number of edges is greater than  $2v - 3$ .

The crucial difference between spherical embedded graphs and planar tilings is that on the sphere there exist *pseudodigons*, that is, spherical polygons with exactly two convex angles. Therefore, a pointed tiling of the sphere may contain pseudodigons, which changes the counts from the Euler formula, and as a consequence there are pointed graphs on the sphere that have non-zero stress. Such a graph should have at least four pseudodigons, and the other tiles must be pseudotriangles. Then we know from Lemma 26 that the graph gives a hyperbolic virtual polytope. This enables us to construct hyperbolic virtual polytopes by just drawing pointed graphs on the sphere.

**6.2. Valuations of virtual polytopes. Volume and count of integer points.**

A *valuation* is a real-valued function  $\varphi: \mathcal{P} \rightarrow \mathbb{R}$  defined on convex polytopes which is additive: whenever  $K_1, K_2$  and  $K_1 \cup K_2$  are convex polytopes, we have

$$\varphi(K_1 \cup K_2) = \varphi(K_1) + \varphi(K_2) - \varphi(K_1 \cap K_2).$$

A *lattice valuation* is defined only for lattice polytopes, that is, for polytopes whose vertices lie in the standard lattice  $\mathbb{Z}^n \subset \mathbb{R}^n$ . In this survey we consider only *translation-invariant valuations*, that is, valuations which coincide on a polytope and a translate of it.

A valuation  $\varphi$  extends uniquely by linearity to the elements of the algebra of polytopal functions (introduced in § 4.1). Namely, for a function

$$f = \sum \alpha_i I_{K_i}$$

we set

$$\varphi(f) = \sum \alpha_i \varphi(K_i).$$

Thus, it make sense to speak of the *valuation  $\varphi$  of a virtual polytope*, since a virtual polytope has a representation as a polytopal function.

We first discuss the most common example of a valuation, namely, the volume.

*Volume of a virtual polytope.* The volume of a virtual polytope represented by a polytopal function  $f$  obviously equals

$$\int_{\mathbb{R}^n} f(x) dx,$$

where the integration is with respect to Lebesgue measure.

From Fig. 16 one concludes that the volume of a virtual polytope may be negative, and that the volume of a virtual polytope may be zero even if the polytope is not degenerate.

*Count of lattice points for virtual polytopes.* Another important example of a translation-invariant valuation is the number of integer points in the polytope. The lattice points in convex polytopes are a classical object of study: starting from the (old and classical) Pick theorem (see, for instance, [9] and [37]), up to such contemporary applications as calculating the Kontsevich volume (see [38]), lattice points appear systematically in many mathematical and computational problems.

From this valuation on lattice polytopes we proceed to the notion of the *number of (weighted) lattice points in a virtual polytope*: for a virtual polytope represented by a polytopal function  $f$ , we define

$$Q(f) = \sum_{x \in \mathbb{Z}^n} f(x).$$

For a convex polytope  $K$ , all the weights equal 1 for all the points in  $K$ . For a virtual polytope, the values of the weights are the values of the polytopal function  $f$  (see Fig. 45 for an example).

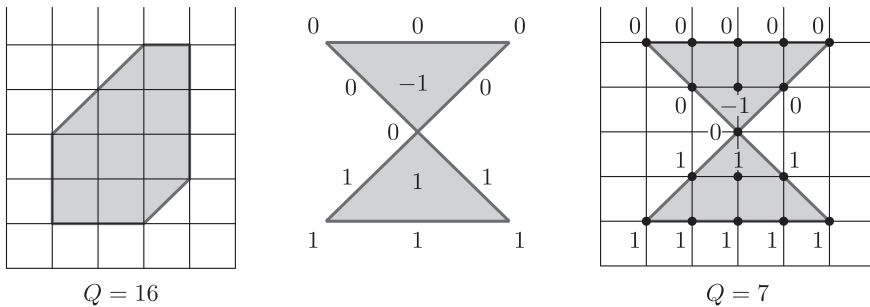


Figure 45. Integer points in a convex polytope and in a virtual polytope.

*Valuations: general case.* Now we go back to all possible valuations, keeping in mind the above two particular examples. McMullen observed in [39] that each valuation behaves polynomially with respect to Minkowski addition.

**Theorem 30.** *Let  $K_1, \dots, K_n \subset \mathbb{R}^n$  be convex polytopes. For a valuation  $\varphi$  and non-negative numbers  $\lambda_1, \dots, \lambda_n$ , the function*

$$P_\varphi(\lambda_1, \dots, \lambda_n) = \varphi((\lambda_1)K_1 \otimes \dots \otimes (\lambda_n)K_n)$$

*is a polynomial in the variables  $\lambda_1, \dots, \lambda_n$ .*

*In the case of lattice polytopes a similar statement is true for non-negative integers  $\lambda_1, \dots, \lambda_n$  and for convex lattice polytopes.*

If we apply the theorem for the volume valuation  $V$ , we arrive at the classical notion of mixed volumes.

**Definition 19.** In the notation of Theorem 30 with  $\varphi = V$ , the coefficient of the polynomial  $P_\varphi = P_V$  at the monomial  $\lambda_1 \cdots \lambda_n$  is called the *mixed volume of the polytopes*  $K_1, \dots, K_n$  and is denoted by  $V(K_1, \dots, K_n)$ .

We emphasize that initially Theorem 30 is only applicable to convex polytopes and positive dilations. Virtual polytope theory gives an elegant answer to the intriguing question of *what*  $P_\varphi(\lambda_1, \dots, \lambda_n)$  *means for arbitrary (not all positive)*  $\lambda_1, \dots, \lambda_n$ . The first observation in this direction is due to McMullen.

**Theorem 31** ([39]). *Let  $K_1 = K_2 = \cdots = K_n = K$  be a convex polytope, and let  $P_\varphi$  be the polynomial in Theorem 30. Then*

$$P_\varphi(-1) = \sum_F (-1)^{\dim F} \varphi(F),$$

where the sum extends over all faces of  $K$  including  $K$  itself.

This theorem can be reformulated in terms of virtual polytopes.

**Theorem 32.** *In the notation of Theorem 31,*

$$P_\varphi(-1) = \varphi(K^{\otimes -1}),$$

where  $K^{\otimes -1}$  is the Minkowski inverse of the polytope  $K$ .

For  $\varphi = Q$  this formula becomes

$$P_Q(-1) = (-1)^{\dim K} \cdot (\text{the number of lattice points strictly inside } K),$$

which is *Ehrhart's reciprocity law* (see [40]).

Pukhlikov and Khovanskii proved a more general fact which covers both McMullen's theorem and Ehrhart's reciprocity law. Namely, they proved that Theorem 30 is valid for arbitrary virtual polytopes and arbitrary real coefficients. To formulate this theorem, we first define the *Minkowski power of a virtual polytope*.

Observe that for a virtual polytope  $K$  and a positive integer  $\lambda$ , the Minkowski power

$$K^{\otimes \lambda} = \underbrace{K \otimes \cdots \otimes K}_\lambda$$

equals the dilation of the polytope  $K$  by  $\lambda$ . This motivates the following.

**Definition 20** (Minkowski power of a virtual polytope). For a positive (not necessarily integer)  $\lambda$  and a virtual polytope  $K$ , we define  $K^{\otimes \lambda}$  to be the dilation of  $K$  by  $\lambda$ :

$$K^{\otimes \lambda} = (\lambda)K.$$

For a negative  $\lambda$  and for a virtual polytope  $K$ , we define

$$K^{\otimes \lambda} = (-\lambda)K^{\otimes -1}.$$

This definition lets us formulate the next theorem.

**Theorem 33** ([1]). *Let  $K_1, \dots, K_n \subset \mathbb{R}^n$  be virtual polytopes. For a valuation  $\varphi$  that is translation invariant and for any real numbers  $\lambda_1, \dots, \lambda_n$ , the function*

$$P_\varphi(\lambda_1, \dots, \lambda_n) = \varphi(K_1^{\otimes \lambda_1} \otimes \dots \otimes K_n^{\otimes \lambda_n})$$

*is a polynomial in the variables  $\lambda_1, \dots, \lambda_n$ .*

*The same is true for a lattice valuation, for lattice virtual polytopes, and for integers  $\lambda_1, \dots, \lambda_n$ .*

This theorem allows us to define mixed volumes for virtual polytopes by literally repeating Definition 19.

**Definition 21.** In the notation of the above theorem applied for the volume valuation  $V$ , the coefficient of the polynomial  $P_V$  at the monomial  $\lambda_1 \cdots \lambda_n$  is called the mixed volume of the virtual polytopes  $K_1, \dots, K_n$  and is denoted by  $V(K_1, \dots, K_n)$ .

The above construction fits nicely the paradigm that *virtual polytopes retain all the properties and structures of convex polytopes except for convexity.*

*Historical remarks.* The special case of Theorem 30 with the volume taken as a valuation was known long before McMullen’s work: Minkowski used the corresponding fact when defining mixed volumes. This concept became the central part of the Brunn–Minkowski theory (details can be found in many textbooks, for instance, [8]). Algorithmic aspects of an efficient enumeration of lattice points in polytopes are treated in [41], which also explains the connection between the number of integer points and the Todd class of the toric variety, a topic beyond the scope of the present survey. However, we mention very briefly that the classical Euler–Maclaurin formula (which involves lattice points on a segment) extends to lattice points and convex polytopes and then to virtual polytopes. This was developed in [42] and further generalized in [43].

**6.3. Mixed volumes of virtual polytopes.** We have defined mixed volumes for virtual polytopes in Definition 21. However, mixed volumes can be extended by linearity even further, namely, to the set of all polytopal functions (see [3] and [44]).

**Definition 22.** For a polytopal function  $f = \sum \alpha_i I_{K_i}$  we define the mixed volume by setting

$$V(f, *, \dots, *) := \sum \alpha_i V(K_i, *, *, \dots, *),$$

where  $*$  stands for arbitrary polytopal functions.

We say that two polytopal functions  $f$  and  $f'$  have the *same behaviour with respect to mixed volume* if for any polytopal functions  $g_1, \dots, g_{n-1}$

$$V(f, g_1, \dots, g_{n-1}) = V(f', g_1, \dots, g_{n-1}).$$

It is known that a convex polytope can be uniquely reconstructed by its behavior with respect to mixed volume calculation. The same holds true for virtual polytopes.

**Theorem 34** ([10]). *Two virtual polytopes have the same behaviour with respect to mixed volume if and only if they coincide.*

In both convex and virtual settings, the proof is based on the fact that mixed volume calculation reduces to a formula for  $V(f, g_1, \dots, g_{n-1})$  involving the support function of the (virtual) polytope  $f$ .

However, the theorem holds just for virtual polytopes, and not for arbitrary polytopal functions. A natural question arises: *To what extent is a polytopal function determined by its behaviour with respect to mixed volume?*

To answer the question, we need some preliminary constructions. Define a map  $\Xi$  from the polytopal functions to virtual polytopes by setting

$$\Xi\left(\sum \alpha_i I_{K_i}\right) = \bigotimes_i K_i^{\otimes \alpha_i}.$$

Here  $K_i^{\otimes \alpha_i}$  is the Minkowski power (see Definition 20). The definition of the map  $\Xi$  is correct, that is, the right-hand side does not depend on the representation of  $f$  as a linear combination. Here is one simple but important consequence of the correctness of the definition.

**Proposition 35.** *Assume that the characteristic function of some convex polytope  $K$  is decomposed as  $I_K = \sum_i \alpha_i I_{K_i}$ , where the  $K_i$  are some convex polytopes. Then*

$$K = \bigotimes_i K_i^{\otimes \alpha_i}.$$

With the above definition, we can now formulate the following proposition.

**Proposition 36** ([10]). *A polytopal function  $f$  and the virtual polytope  $\Xi(f)$  have the same behaviour with respect to mixed volume.*

Combined with Theorem 34, this immediately gives the following theorem.

**Theorem 37** ([10]). *Two polytopal functions  $f$  and  $g$  have the same behaviour with respect to mixed volume if and only if the associated virtual polytopes  $\Xi(f)$  and  $\Xi(g)$  coincide.*

**6.4. Minkowski decomposition of polytopes.** The question raised below is motivated by the theory of zonotopes. A *zonotope* is a convex polytope decomposable into a Minkowski sum of line segments [45]. Zonotopes appear in surprisingly diverse areas of mathematics ranging from classical convexity to universality theorems [46], (oriented) matroids [47], and many others. A nice property of zonotopes is that they can be easily characterized: a polytope is a zonotope if and only if all its two-dimensional faces are centrally symmetric. The summands of a zonotope are also easily recovered: they are the edges of the zonotope. The faces of a zonotope are also zonotopes.

The question of characterizing the polytopes which can be decomposed into a Minkowski sum of polytopes of a certain fixed lower dimension arises in a natural way. In this subsection we discuss the following question: *Given a  $d$ -dimensional convex polytope, can it be represented as a Minkowski sum of  $(d - 1)$ -dimensional virtual polytopes? And if yes, then find such a representation.*

The answer is as follows: an  $n$ -dimensional convex polytope is representable as a sum of  $(n - 1)$ -dimensional virtual polytopes (or equivalently, as a weighted sum of  $(n - 1)$ -dimensional convex polytopes) if and only if it equals the Minkowski sum of its faces  $F$  taken with certain prescribed weights  $w_F$ .

Now we make this precise. Let a convex polytope  $K$  in  $\mathbb{R}^n$  be represented by its characteristic function  $I_K$  (see § 4.1), and let

$$J_K(x) = \lim_{\varepsilon \rightarrow 0} \frac{1}{V_\varepsilon} \int_{B_\varepsilon(x)} I_K(t) dt,$$

where  $B_\varepsilon(x)$  is the ball of radius  $\varepsilon$  about the point  $x$ ,  $V_\varepsilon$  is its volume, and the integration is with respect to Lebesgue measure.

The function  $J_K(x)$  is clearly a polytopal function. Indeed, it is constant on the relative interiors of the faces of  $K$ , and therefore it decomposes as a weighted sum of characteristic functions of the faces:

$$J_K(x) = \sum_F w_F I_F(x),$$

where the sum is over all the faces of  $K$ , including  $K$  itself.

For instance, we always have  $w_K = 1$ , and  $w_F = -1/2$  for a facet  $F$ . The other weights depend on the angular measures of the polytope  $K$  (see, for example, Fig. 46).

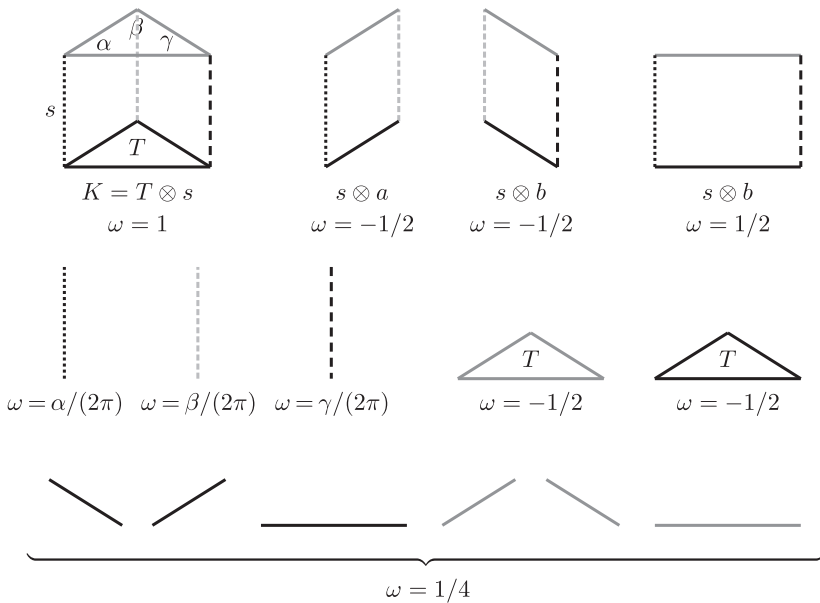


Figure 46. A prism decomposes into the sum of its faces.

**Theorem 38** ([12]). *Let  $K$  be a convex polytope. In the notation introduced above and that in Definition 20,  $K$  is representable as a sum of  $(d-1)$ -dimensional virtual polytopes if and only if*

$$\bigotimes_F F^{\otimes w_F} = E, \tag{5}$$

where the sum is over all faces of  $K$ , including  $K$  itself, and  $E$  is the one-point polytope, that is, the unit element of the group of virtual polytopes.

If the equality (5) holds, then

$$K = \bigotimes_F F^{\otimes -w_F},$$

where the sum is over all proper faces of  $K$ , that is, all faces excluding  $K$ . (This is the required representation of  $K$  by a Minkowski sum of lower-dimensional polytopes.)

**Example 18.** A convex tetrahedron in  $\mathbb{R}^3$  is not representable as a sum of planar virtual polytopes.

**Example 19.** Let us see how the theorem works for a prism  $K = T \otimes s$ , which is the Minkowski sum of a triangle  $T$  and a segment  $s$ . Figure 46 lists all the faces of the prism  $K$  together with their weights. After reduction, we have

$$\bigotimes_F F^{\otimes w_F} = K \otimes s^{\otimes -1} \otimes T^{\otimes -1} = E.$$

Therefore,  $K = T \otimes s$ .

Theorem 38 implies by induction similar results for decomposing a  $d$ -polytope into a Minkowski sum of virtual  $k$ -polytopes for all  $k < d$ .

**6.5. Projective toric varieties, Picard group, and Riemann–Roch Theorem.** We conclude our survey by expounding briefly on the relation between projective toric varieties and virtual polytopes. This was the starting point which motivated Khovanskii and Pukhlikov [1].

Projective toric varieties form an important class of examples in algebraic geometry. The name ‘toric’ is used because a toric variety contains an algebraic torus as an open dense subset, and the natural action of the torus on itself extends to the entire variety. A projective toric variety is determined by the underlying fan, which is the outer normal fan of some lattice convex polytope. For example, the complex projective space  $\mathbb{C}P^n$  (which is a toric variety) is associated in this sense to the  $n$ -dimensional simplex.

There exists a kind of ‘dictionary’ which translates many algebraic geometry notions and theorems into notions and theorems in the geometry of convex polytopes. Among others, these are: singularities, morphisms, intersection theory, Hodge inequality, the Riemann–Roch theorem. As a consequence, general facts from algebraic geometry have implications to polytopes, and vice versa. Virtual polytopes fit this framework nicely: the dictionary translates them as elements of the *Picard group*, that is, *invertible sheaves*, whereas convex polytopes are translated as *very ample sheaves*.

*Projective toric varieties. A brief overview.* For a detailed presentation, see [48], [9], and [21].

For a convex rational simple polytope let  $\Sigma$  be an outer normal fan whose cones are *regular* (regularity is some additional property) in  $\mathbb{R}^n$ . Let  $\sigma \in \Sigma$  be these cones and let  $\check{\sigma}$  be their dual cones. We associate to it a projective toric variety  $X_\Sigma$  obtained from  $\Sigma$  by the following construction.

- *Laurent polynomials.* Take the algebra of Laurent polynomials over  $\mathbb{C}$  in  $n$  variables:

$$\mathbb{C}[\mathbf{z}, \mathbf{z}^{-1}] = \left\{ \sum_{\mathbf{a}} \lambda_{\mathbf{a}} \mathbf{z}^{\mathbf{a}} = \sum_{(a_1, \dots, a_n)} \lambda_{(a_1, \dots, a_n)} z_1^{a_1} z_2^{a_2} \cdots z_n^{a_n} \right\},$$

where  $\mathbf{a} = (a_1, \dots, a_n) \in \mathbb{Z}^n$ , and the coefficients  $\lambda_{\mathbf{a}}$  are complex numbers. The support of a Laurent polynomial is defined as

$$\text{supp}\left(\sum \lambda_{\mathbf{a}} \mathbf{z}^{\mathbf{a}}\right) = \{\mathbf{a} : \lambda_{\mathbf{a}} \neq 0\}.$$

- *Defining charts.* Each cone  $\sigma$  in the fan  $\Sigma$  yields the algebra  $R_{\check{\sigma}}$  of Laurent polynomials with support in the dual cone:

$$R_{\check{\sigma}} := \{f \in \mathbb{C}[z, z^{-1}] : \text{supp}(f) \subset \check{\sigma}\}.$$

Next, we define the affine algebraic variety (chart)  $X_{\check{\sigma}}$  as the maximal spectrum of  $R_{\check{\sigma}}$ .

- *Gluing charts together.* The following observation lets us define gluing maps between the charts  $X_{\check{\sigma}}$ . Suppose that  $\tau$  is a face of  $\sigma$ , where  $\tau, \sigma \in \Sigma$ . Then we have  $\check{\tau} \supset \check{\sigma}$ , which implies a natural inclusion of algebras  $R_{\check{\sigma}} \rightarrow R_{\check{\tau}}$ , and consequently an inclusion of affine algebraic varieties  $X_{\check{\tau}} \rightarrow X_{\check{\sigma}}$ . In other words, we have an identification of  $X_{\check{\tau}}$  as a subset of  $X_{\check{\sigma}}$ .

The collection of all charts  $X_{\check{\sigma}}$ , together with gluing maps, yields a smooth projective algebraic variety  $X_\Sigma$ . Because of some extra structure (it contains a dense embedded torus which acts on  $X_\Sigma$ ), it is called a *toric variety*.

- *Structure sheaf.* The collection of algebras  $\{R_{\check{\sigma}}\}$  yields a sheaf of algebras on  $X_\Sigma$  called the *structure sheaf*  $\mathcal{O}_{X_\Sigma}$ .

*Picard group of  $X_\Sigma$  and the lattice combinatorial Picard group.* The variety  $X_\Sigma$  comes with its *Picard group*, which is the set of isomorphic classes of invertible sheaves of  $\mathcal{O}_{X_\Sigma}$ -modules. The group operation for invertible sheaves is the tensor product  $\otimes$ , and the unit element in the Picard group is  $\mathcal{O}_{X_\Sigma}$ .

Let  $K$  be a lattice virtual polytope, that is, a virtual polytope whose vertices lie on the standard lattice  $\mathbb{Z}^n$ . We assume in addition that the fan  $\Sigma_K$  is coarser than  $\Sigma$ . We represent  $K$  as an element of the combinatorial Picard group, that is, as a system of translated cones  $p_\sigma \otimes \check{\sigma}$  (see § 4.4), and we define an invertible sheaf  $\mathcal{F}_K$  of  $\mathcal{O}_{X_\Sigma}$ -modules on  $X_\Sigma$  by setting

$$\mathcal{F}_K(X_{\check{\sigma}}) = z^{p_\sigma} \mathcal{O}_{X_\Sigma}(X_{\check{\sigma}}).$$

**Theorem 39** ([9]). *The map  $K \rightarrow \mathcal{F}_K$  establishes an isomorphism between the lattice combinatorial Picard group  $\mathcal{CP}_\Sigma^{\mathbb{Z}}$  and the Picard group of the projective toric variety  $X_\Sigma$ .*

Let us now pass from the group of virtual polytopes related to one particular fan to the whole group of lattice virtual polytopes.

We have already noted in § 4.4 that for a given fan  $\Sigma$  and a refinement  $\Sigma'$  of it there is a natural inclusion for the groups of lattice virtual polytopes related to these fans:  $\mathcal{P}_{\mathbb{Z},\Sigma}^* \subseteq \mathcal{P}_{\mathbb{Z},\Sigma'}^*$ .

Furthermore, there is a natural toric epimorphism  $X_{\Sigma'} \rightarrow X_\Sigma$  which in turn induces an inclusion of the Picard groups:  $\text{Pic}(X_\Sigma) \subseteq \text{Pic}(X_{\Sigma'})$ .

This enables us to speak of the *inductive limits* of the groups  $\mathcal{P}_{\mathbb{Z},\Sigma}^*$  and  $\text{Pic}(X_\Sigma)$ . Thus, the inductive limit in Theorem 39 yields the following theorem.

**Theorem 40.** *The group  $\mathcal{P}_{\mathbb{Z},\Sigma}^*$  of lattice virtual polytopes is isomorphic to the inductive limit of the Picard groups  $\text{Pic}(X_\Sigma)$ .*

*Riemann–Roch theorem and enumeration of integer points.* Here is one more nice observation from [49]: Theorem 30 for the valuation  $Q$  (which counts integer points) follows from the Riemann–Roch theorem for toric varieties (see [50]).

The argument proceeds by translating Theorem 30 into the language of toric varieties: a polytope  $K$  is translated as an invertible sheaf, and the number of lattice points in  $K$  is translated as the value of the Euler characteristic with coefficients in the invertible sheaf corresponding to  $K$ . It remains to apply the Riemann–Roch theorem, which says that the Euler characteristic behaves polynomially with respect to the tensor product: the function  $n \rightarrow \xi(X_\Sigma, \mathcal{F}_K^{\otimes n})$  is a polynomial in  $n$ . It can be checked that for convex polytopes the value of this polynomial equals the number of lattice points.

### 7. Concluding remarks

The theory of virtual polytopes presented in this survey started with the very simple algebraic passage from the semigroup of convex polytopes with Minkowski addition to its associated Grothendieck group. However, the core of the theory lies in the many geometric representations of virtual polytopes, together with the canonical isomorphisms between different representations, and also in their applications.

Different problems make use of one or another of these representations, as appropriate for the particular problem. For example, the Minkowski decomposition problem in § 6.4 relied on the polytopal function representation in § 4.1. And for solving Alexandrov’s problem discussed in § 6.1, the techniques in § 5.1 involving spherical stressed graphs were used in combination with ideas in § 5.5 concerning support functions.

An important conclusion to be extracted from this survey is that virtual polytopes possess all the properties and structures of convex polytopes, except of course convexity. But the partially ordered set of faces, the mixed volumes, the theory of enumeration of lattice points, and other notions have natural generalizations to this extended class of polytopes.

Geometrically, virtual polytopes may sometimes appear to be counterintuitive: we have seen examples of hyperbolic polytopes with an everywhere saddle support function in §6.1, examples of a 3D virtual polytope whose vertex-edge graph is not 3-connected in Example 15 and Figure 39, a flexible virtual polytope in Example 16 and Figure 40, and other examples not encountered in the world of convex polytopes.

We hope that by the end of this survey the reader will have found, as we did, that virtual polytopes are interesting objects of study in their own right, and we anticipate that further applications will emerge in the future (including some of a computational nature).

## Bibliography

- [1] A. В. Пухликов, А. Г. Хованский, “Конечно-аддитивные меры виртуальных многогранников”, *Алгебра и анализ* 4:2 (1992), 161–185; english transl., A. V. Pukhlikov and A. G. Khovanskii, “Finitely additive measures of virtual polytopes”, *St. Petersburg Math. J.* 4:2 (1993), 337–356.
- [2] A. D. Alexandroff (Alexandrov), “Sur les théorèmes d’unicité pour les surfaces fermées”, *Докл. АН СССР* 22:3 (1939), 99–102.
- [3] H. Groemer, “Minkowski addition and mixed volumes”, *Geometriae Dedicata* 6:2 (1977), 141–163.
- [4] L. Rodríguez and H. Rosenberg, “Rigidity of certain polyhedra in  $\mathbf{R}^3$ ”, *Comment. Math. Helv.* 75:3 (2000), 478–503.
- [5] V. Alexandrov, “Minkowski-type and Alexandrov-type theorems for polyhedral herissons”, *Geom. Dedicata* 107 (2004), 169–186.
- [6] Y. Martinez-Maure, “Théorie des hérissons et polytopes”, *C. R. Math. Acad. Sci. Paris* 336:3 (2003), 241–244.
- [7] P. McMullen, “The polytope algebra”, *Adv. Math.* 78:1 (1989), 76–130.
- [8] R. Schneider, *Convex bodies: the Brunn–Minkowski theory*, Encyclopedia Math. Appl., vol. 44, Cambridge Univ. Press, Cambridge 1993, xiv+490 pp.
- [9] G. Ewald, *Combinatorial convexity and algebraic geometry*, Grad. Texts in Math., vol. 168, Springer-Verlag, New York 1996, xiv+372 pp.
- [10] Г. Ю. Панина, “Виртуальные многогранники и классические вопросы геометрии”, *Алгебра и анализ* 14:5 (2002), 152–170; English transl., G. Yu. Panina, “Virtual polytopes and classical questions in geometry”, *St. Petersburg Math. J.* 14:5 (2003), 823–834.
- [11] O. Ya. Viro, “Some integral calculus based on Euler characteristic”, *Topology and geometry – Rohlin seminar*, Lecture Notes in Math., vol. 1346, Springer, Berlin 1988, pp. 127–138.
- [12] Г. Ю. Панина, “Структура группы виртуальных многогранников относительно подгрупп цилиндров”, *Алгебра и анализ* 13:3 (2001), 179–197; English transl., G. Yu. Panina, “The structure of the virtual polytope group relative to cylinder subgroups”, *St. Petersburg Math. J.* 13:3 (2002), 471–484.
- [13] P. McMullen, “Separation in the polytope algebra”, *Beiträge Algebra Geom.* 34:1 (1993), 15–30.
- [14] W. Fulton and B. Sturmfels, “Intersection theory on toric varieties”, *Topology* 36:2 (1997), 335–353.
- [15] M. Brion, “The structure of the polytope algebra”, *Tohoku Math. J. (2)* 49:1 (1997), 1–32.

- [16] R. P. Stanley, “The number of faces of a simplicial convex polytope”, *Adv. in Math.* **35**:3 (1980), 236–238.
- [17] P. McMullen, “On simple polytopes”, *Invent. Math.* **113** (1993), 419–444.
- [18] В. А. Тиморин, “Аналог соотношений Ходжа–Римана для простых выпуклых многогранников”, *УМН* **54**:2(326) (1999), 113–162; English transl., V. A. Timorin, “An analogue of the Hodge–Riemann relations for simple convex polytopes”, *Russian Math. Surveys* **54**:2 (1999), 381–426.
- [19] В. М. Бухштабер, “Кольцо простых многогранников и дифференциальные уравнения”, *Геометрия, топология и математическая физика. I*, Сборник статей. К 70-летию со дня рождения академика Сергея Петровича Новикова, Тр. МИАН, **263**, МАИК, М. 2008, с. 18–43; English transl., V. M. Buchstaber, “Ring of simple polytopes and differential equations”, *Proc. Steklov Inst. Math.* **263** (2008), 13–37.
- [20] В. М. Бухштабер, Н. Ю. Ероховец, “Многогранники, числа Фибоначчи, алгебры Хопфа и квазисимметрические функции”, *УМН* **66**:2(398) (2011), 67–162; English transl., V. M. Buchstaber and N. Yu. Erokhovets, “Polytopes, Fibonacci numbers, Hopf algebras, and quasi-symmetric functions”, *Russian Math. Surveys* **66**:2 (2011), 271–367.
- [21] Т. Oda, *Convex bodies and algebraic geometry. An introduction to the theory of toric varieties*, *Ergeb. Math. Grenzgeb.* (3), vol. 15, Springer-Verlag, Berlin 1988, viii+212 pp.
- [22] G. Panina, “On hyperbolic virtual polytopes and hyperbolic fans”, *Cent. Eur. J. Math.* **4**:2 (2006), 270–293.
- [23] G. Yu. Panina, “Pointed spherical tilings and hyperbolic virtual polytopes”, *Геометрия и топология. 11*, Зап. науч. сем. ПОМИ, **372**, ПОМИ, СПб. 2009, с. 157–171; *J. Math. Sci. (N. Y.)* **175**:5 (2011), 591–599.
- [24] G. Panina, “New counterexamples to A. D. Alexandrov’s hypothesis”, *Adv. Geom.* **5**:2 (2005), 301–317.
- [25] C. J. Brianchon, “Théorème nouveau sur les polyèdres”, *J. Ecole (Royale) Polytechnique* **15** (1837), 317–319.
- [26] J. C. Maxwell, “On reciprocal figures, frames, and diagrams of forces”, *Trans. R. Soc. Edinburgh* **26**:1 (1870), 1–40.
- [27] G. M. Ziegler, *Lectures on polytopes*, *Grad. Texts in Math.*, vol. 152, Springer-Verlag, New York 1995, x+370 pp.
- [28] Y. Martinez-Maure, “Contre-exemple à une caractérisation conjecturée de la sphère”, *C. R. Acad. Sci. Paris Sér. I Math.* **332**:1 (2001), 41–44.
- [29] M. Knyazeva and G. Panina, “An illustrated theory of hyperbolic virtual polytopes”, *Cent. Eur. J. Math.* **6**:2 (2008), 204–217.
- [30] M. Knyazeva and G. Panina, *A counterexample to A. D. Alexandrov’s conjecture*, EG-Models – archive of electronic geometry models, model № 2010.02.002, 2010, [http://www.eg-models.de/models/Surfaces/2010.02.002/\\_preview.html](http://www.eg-models.de/models/Surfaces/2010.02.002/_preview.html).
- [31] G. Panina, “A. D. Alexandrov’s uniqueness theorem for convex polytopes and its refinements”, *Beiträge Algebra Geom.* **49**:1 (2008), 59–70.
- [32] G. Panina, “Around A. D. Alexandrov’s uniqueness theorem for convex polytopes”, *Adv. Geom.* **12**:4 (2012), 621–637.
- [33] G. Rote, F. Santos, and I. Streinu, “Pseudo-triangulations – a survey”, *Surveys on discrete and computational geometry. Twenty years later*, *Contemp. Math.*, vol. 453, Amer. Math. Soc., Providence, RI 2008, pp. 343–410; 2006 (v2 – 2007), 68 pp., arXiv:math/0612672.

- [34] I. Streinu, “A combinatorial approach to planar non-colliding robot arm motion planning”, *41st Annual Symposium on Foundations of Computer Science* (Redondo Beach, CA 2000), IEEE Comput. Soc. Press, Los Alamitos, CA 2000, pp. 443–453.
- [35] I. Streinu, “Pseudo-triangulations, rigidity and motion planning”, *Discrete Comput. Geom.* **34**:4 (2005), 587–635.
- [36] G. A. Pick, “Geometrisches zur Zahlenlehre”, *Sonderabdr. Naturw.-medizin. Verein f. Böhmen ‘Lotos’* **19** (1899), 311–319.
- [37] B. Grünbaum, *Convex polytopes*, Pure and Applied Mathematics, vol. 16, Interscience Publishers John Wiley & Sons, Inc., New York 1967, xiv+456 pp.
- [38] P. Norbury, “Counting lattice points in the moduli space of curves”, *Math. Res. Lett.* **17**:3 (2010), 467–481; 2008, 15 pp., arXiv:0801.4590.
- [39] P. McMullen, “Valuations and Euler-type relations on certain classes of convex polytopes”, *Proc. London Math. Soc.* (3) **35**:1 (1977), 113–135.
- [40] E. Ehrhart, *Polynômes arithmétiques et méthode des polyèdres en combinatoire*, Internat. Ser. Numer. Math., vol. 35, Birkhäuser Verlag, Basel–Stuttgart 1977, 165 pp.
- [41] A. Barvinok and J. E. Pommersheim, “An algorithmic theory of lattice points in polyhedra”, *New perspectives in algebraic combinatorics* (Berkeley, CA 1996–97), Math. Sci. Res. Inst. Publ., vol. 38, Cambridge Univ. Press, Cambridge 1999, pp. 91–147.
- [42] А. В. Пухликов, А. Г. Хованский, “Теорема Римана–Роха для интегралов и сумм квазиполиномов по виртуальным многогранникам”, *Алгебра и анализ* **4**:4 (1992), 188–216; English transl., A. V. Pukhlikov and A. G. Khovanskii, “The Riemann–Roch theorem for integrals and sums of quasipolynomials on virtual polytopes”, *St. Petersburg Math. J.* **4**:4 (1993), 789–812.
- [43] M. Brion and M. Vergne, “Lattice points in simple polytopes”, *J. Amer. Math. Soc.* **10**:2 (1997), 371–392.
- [44] Г. Ю. Панина, “Смешанные объемы невыпуклых тел”, *Изв. НАН Армении. Матем.* **28**:1 (1993), 72–81; English transl., G. Yu. Panina, “Mixed volumes for nonconvex bodies”, *J. Contemp. Math. Anal.* **28**:1 (1993), 63–71.
- [45] R. Schneider and W. Weil, “Zonoids and related topics”, *Convexity and its applications*, Birkhäuser, Basel 1983, pp. 296–317.
- [46] J. Richter-Gebert, *Realization spaces of polytopes*, Lecture Notes in Math., vol. 1643, Springer-Verlag, Berlin 1996, xii+187 pp.
- [47] A. Björner, M. Las Vergnas, B. Sturmfels, N. White, and G. M. Ziegler, *Oriented matroids*, 2nd ed., Encyclopedia Math. Appl., vol. 46, Cambridge 1999, xii+548 pp.
- [48] В. И. Данилов, “Геометрия торических многообразий”, *УМН* **33**:2(200) (1978), 85–134; English transl., V. I. Danilov, “The geometry of toric varieties”, *Russian Math. Surveys* **33**:2 (1978), 97–154.
- [49] А. Г. Хованский, “Многогранники Ньютона и торические многообразия”, *Функц. анализ и его прил.* **11**:4 (1977), 56–64; English transl., A. G. Khovanskii, “Newton polyhedra and toroidal varieties”, *Funct. Anal. Appl.* **11**:4 (1977), 289–296.
- [50] F. Hirzebruch, *Neue topologische Methoden in der algebraischen Geometrie*, 2. erg. Aufl., *Ergeb. Math. Grenzgeb.* (N. F.), vol. 9, Springer-Verlag, Berlin–Göttingen–Heidelberg 1962, vii+181 pp.; English transl., F. Hirzebruch,

*Topological methods in algebraic geometry*, 3rd ed., Grundlehren Math. Wiss.,  
vol. 131, Springer-Verlag, New York 1966, x+232 pp.

**Gayanè Yu. Panina**

St. Petersburg State University;  
St. Petersburg Institute for Informatics and  
Automation of the Russian Academy of Sciences  
*E-mail:* [gaiane-panina@rambler.ru](mailto:gaiane-panina@rambler.ru)

Received 10/DEC/14  
Translated by G. PANINA

**Ileana Streinu**

Department of Computer Science, Smith College,  
Northampton, MA, USA  
*E-mail:* [istreinu@smith.edu](mailto:istreinu@smith.edu)